INVESTIGATING IMPACT OF MYCOBACTERIAL PHYSIOLOGY ON

MYCOBACTERIOPHAGE LIFE CYCLES BY MASS SPECTROMETRY

A Dissertation

Submitted to the Faculty

of

Purdue University

by

Yi Li

In Partial Fulfillment of the

Requirements for the Degree

of

Doctor of Philosophy

December 2018

Purdue University

West Lafayette, Indiana

THE PURDUE UNIVERSITY GRADUATE SCHOOL
STATEMENT OF DISSERTATION APPROVAL

Dr. Kari L. Clase, Chair

> Department of Agricultural and Biological Engineering

Dr. Jenna L. Rickus

> Department of Agricultural and Biological Engineering

Dr. Bruce M. Applegate

> Department of Food Sciences

Dr. Richard J. Kuhn

> Department of Biological Sciences

Approved by:

> Dr. Bernard A. Engel

> > Head of the School Graduate Program

ACKNOWLEDGMENTS

TABLE OF CONTENTS

Page

LIST OF TABLES

LIST OF FIGURES

ABBREVIATIONS

ACN	acetonitrile
AG	arabinogalactan
AHL	acyl-homoserine lactone
ANI	average nucleotide identities
CDC	Centers for Disease Control and Prevention
CID	collision induced dissociation
CL	cardiolipin
DAG	diglyceride
DAT	diacyltrehaloses
DNA	deoxyribonucleic acid
LFQ	label-free quantification
PECAAN	Phage Evidence Collection And Annotation Network
ELISA	Enzyme-Linked Immunosorbent Assay
ESI	electrospray ionization
E. coli	*Escherichia coli*
FA	formic acid
FDA	Food and Drug Administration
GO	Gene Ontology
HHMI	The The Howard Hughes Medical Institute
HPLC	High Performance Liquid Chromatography
LB	Luria-Bertani
LM	lipomannan
LPE	lysohosphatidylethanolamine
LPI	lysophosphatidylinositol

MA	mycolic acid
MAG	monoacylglycero
ManLAM	mannose-capped lipoarabinomannan
MOI	multiplicity of infection
NCBI	The National Center for Biotechnology Information
M. aurum	*Mycobacterium aurum*
M. avium	*Mycobacterium avium*
M. leprae	*Mycobacterium leprae*
M. smegmatis	*Mycobacterium smegmatis*
M. tuberculosis	*Mycobacterium tuberculosis*
P1FF	Passage 1 From the Frozen
P2FF	Passage 2 From the Frozen
PA	phosphatidic acid
PAT	polyacyltrehaloses
PCR	polymerase chain reaction
PDIM	phthiocerol dimycocerosate
PE	phosphatidylethanolamine
PG	peptidoglycan
PGL	phenolic glycolipid
PI	phosphatidylinositol
PIM	phosphatidylinositol mannoside
PS	phosphatidylserine
PSI	pound per square inch
Ptp	phosphotyrosine protein phosphatase
Pup	prokaryotic ubiquitin-like protein
QS	quorum sensing
RNA	ribonucleic acid
rpm	round per minute
rRNA	ribosomal ribonucleic acid

SEA-PHAHES	Science Education Alliance-Phages Hunters Advancing Genomics and Evolutionary Science
SL	sulfolipid
S. enterica	*Salmonella enterica*
TAG	tracylglycerol
TDM	trehalose dimycolate
TEM	transmission electron microscopy
TFA	trifluoroacetic acid
TMM	trehalose monomycolate
tmRNA	transfer ribonucleic acid
tRNA	transfer-messenger ribonucleic acid

NOMENCLATURE

λ phage lambda

CO_2 carbon dioxide

H_2O water

ABSTRACT

Li, Yi Ph.D., Purdue University, December 2018. Investigating Impact of Mycobacterial Physiology on Mycobacteriophage Life Cycles by Mass Spectrometry. Major Professor: Kari L. Clase.

Mycobacteriophages are the viruses that infect mycobacteria. Due to the high death rate and antibiotic-resistant strains, phage therapy is considered to be a promising treatment of tuberculosis. Current understanding of phage-bacteria interaction is abstracted as phage lytic and lysogenic life cycles. However, bacterial physiology may impact phage life cycles and bacterial cells with different physiology may have different responses to phage infection. In order to improve the understanding of phage-bacteria interaction and update phage therapy strategy, the impact of mycobacterial physiology on mycobacteriophage life cycles was studied in this research. In this research, a mass spectrometry-based method was first developed to study phage proteins in phage-bacteria mixture. Then five mycobacteriophages isolated at Purdue University were selected to infect exponential and stationary *Mycobacterium smegmatis* (*M. smegmatis*) cell cultures. Growth curves of the *M. smegmatis* cell cultures infected by the five phages were determined. Proteomics and lipidomics of the *M. smegmatis* cells cultures infected by phages FrenchFry and MrGordo were analyzed by mass spectrometry. The correlations between individual proteins/lipids and the experimental factors (bacterial growth phases, phages and phage infection time) were studied by developing linear regression models using SAS. The mass spectrometry-based method was proved to be able to detect phage proteins other than the structural proteins. It also verified the phage protein annotation that had been accomplished in silico. X! Tandem and a database consisting of six frame translation of the phage genome and the annotated proteins of *M. smegmatis* were the optimal option for analyzing

mass spectra data of phage-bacteria mixture. The growth curves of the *M. smegmatis* infected by the phages displayed that growth of exponential *M. smegmatis* cell cultures were depressed by phages (except FrenchFry) and stationary *M. smegmatis* cell cultures were not actively lysed by any of the phages. The proteomics results showed that MrGrodo infection impacted more proteins than other factors did. Exponential phase up-regulated proteins involved in cell division. Stationary phase up-regulated proteins that may change cell surface properties. FrenchFry up-regulated LuxR protein. Infection time up-regulated the proteins associated with mycobacterial virulence. The lipidomics results indicated that growth phases impacted the most lipids. Phage infection time increased the amount of the lipids related to mycobacterial virulence. In summary, the mass spectrometry-based method developed in this research can be employed to study phage proteins in phage-bacteria mixture and verify phage genome annotation. Mycobacterial physiology alters mycobacteriophage life cycles. Phage-bacteria interaction is the interaction between the two populations instead of between an individual phage particle and an individual bacterial cell. Virulence of *M. smegmatis* improves as a response to phage infection.

1. INTRODUCTION

1.1 Bacteriophage

1.1.1 Introduction of Bacteriophages

Bacteriophages or phages are the viruses that infect certain types of bacteria [1]. Estimated population of phages is over 10^{31} that is about 10 times more than the population of bacteria [2], which makes the phages the most abundant organisms in the world [1]. Lytic activity of phages was observed and depicted in 1890s [3], and phages were then first discovered and identified in 1910s [4, 5]. Phages have various of morphologies (Figure 1.1), including myoviridae, siphoviridae and inoviridae [6]. Similar to other viruses, phage particles consist of two components: a genome of nucleotide material and a capsid made of proteins [7]. Lipids also present in some phages such as PM2 [8] and D29 [9]. The phage genome can either be single- or double-stranded DNA or RNA and is dependent upon the host for replication and the production of new phage particles. Model phages including T4, λ, and M13 that infect *Escherichia coli* (*E. coli*) have been studied in many researches.

1.1.2 Phage Life Cycles

Phage life cycle is selected upon phages attach to host bacterial cells. After injecting genome into host bacterial cells, phages will enter either lytic or lysogenic cycle. In a lytic cycle (Figure 1.2(a)), the phage genome is replicated, transcribed, and translated using the bacterial machinery. Progeny phage particles are then assembled and released out of the bacterial cells. In contrast, during the lysogenic cycle (Figure 1.2(b)), the phage genome is integrated into the bacterial chromosome. Under certain conditions, the integrated phage genome or prophage can be released

Group:	I (dsDNA)	I (dsDNA)	I (dsDNA)	II (ssDNA)	IV (($^+$)ssRNA)
Order:	Caudovirales	Caudovirales	Caudovirales	-	-
Family:	Myoviridae	Siphoviridae	Podoviridae	Inoviridae	Leviviridae
Typical phage:	T4 phage	λphage	T7 phage	M13 phage	MS2 phage
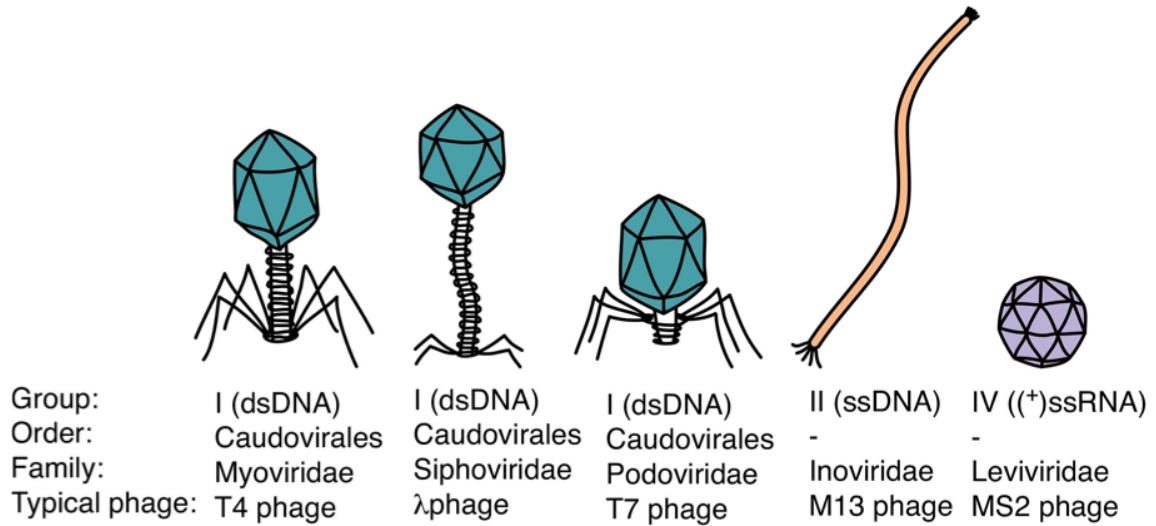
Fig. 1.1. Morphologies of phages [10].

from the host chromosome and subsequently enter a lytic cycle. Besides the lytic and lysogenic cycles, pseudolysogenic cycle in which phage genomes stay inside bacterial cells without further transcription and translation [11], and chronic infection in which progeny phages are release through budding or extrusion instead of lysing bacteria cells [12], are also investigated in previous researches.

1.1.3 Current Application of Phages

Phage therapy

Antibiotics resistant bacteria cause over 2 million infection and 23,000 deaths in the U.S. every year, reported by Centers for Disease Control and Prevention (CDC) [CDC, 2018]. However, development of a new antibiotics may cost over 10 years and billions of dollars [13]. Therefore, phage agents become a promising alternative to antibiotics due to the advantages including antibacterial activity, low inherent toxicity, and low capital cost [14]. Tuberculosis causes over 1.7 millions of deaths

(a) Lytic cycle   (b) Lysogenic cycle
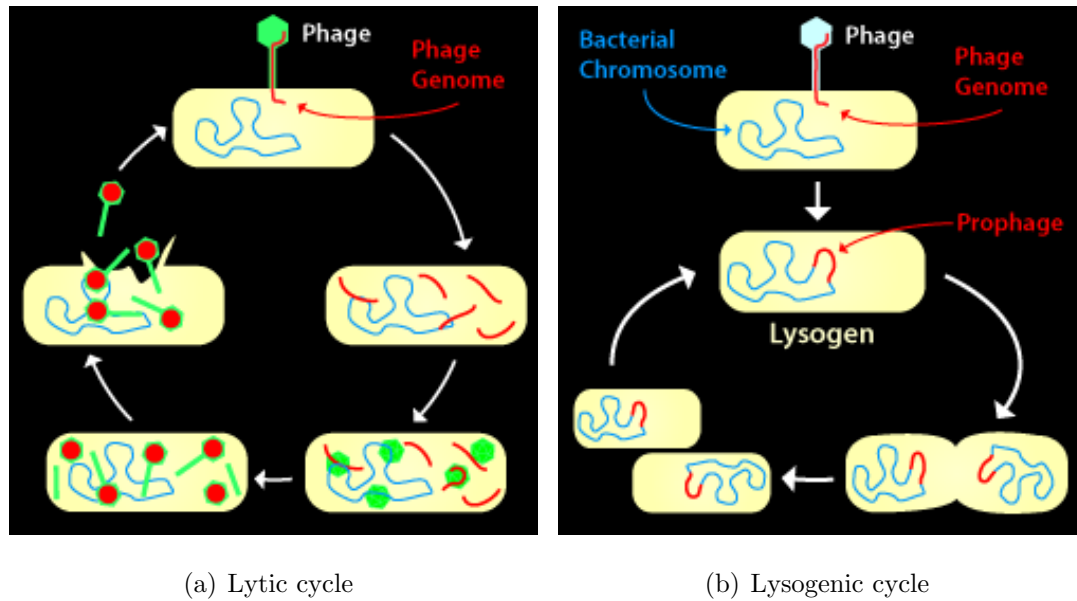
Fig. 1.2. Phage life cycles [The Actinobacteriophage Database, 2018].

per year worldwide [CDC, 2018], and drug-resistance of becomes one of the biggest hurdles to conventional antibiotic treatment [15]. Then phage therapy is considered as an alternative treatment for tuberculosis.

Phages therapy has a long history. In 1919, four dysentery patients were cured by single phage preparation within 48 hours at Hpital des Enfants-Malades in Paris [16], which is the first actual phage therapy case. In 1930, Indiana University School of Medicine conducted a clinical trial with 300 patients using a multi-phage preparation targeting various strains of bacillus and staphylococcus, and about 90% of the patients showed positive results [17]. In 1940s, before the first antibiotics was developed, companies in both France and the U.S. produced phage agents for bacteria such as staphylococci, streptococci and *E. coli*, but these products were not as effective as the fresh phage agents prepared in the lab [16]. Former Soviet Union and eastern Europe showed opener attitude to phage therapy than the U.S. and European countries did, and conducted lots of clinical phage therapy researches [18–20]. Although Food and Drug Administration (FDA) has strict regulatory process for phage agents, phage agents are still considered to be a good alternative to antibiotics in the U.S. [16].

Nano detector for bacteria

Specificity of phage infection makes phages potential detectors for the host bacteria. Conventional detection methods for pathogenic bacteria such as *Salmonella enterica* (*S. enterica*) include culture and at-counting, Enzyme-Linked Immunosorbent Assay (ELISA), biosensors, electrochemistry and polymerase chain reaction (PCR) [21]. These methods all have advantages for different requirements, but they share some mutual disadvantages such as time-consuming and poor sensitivity [21]. A phage-based method was developed [22]. Different from these traditional methods, the bacterial genes encoding luciferase was carried and transduced by phage Felix 01 which lyses all Salmonella strains. This method has high specificity for Salmonella, but the procedures are complicated, and efficiency and detection limits are not tested yet. Inspired by Ulitzur and Kuhn [23], Ripp *et al.* [24] improved the phage-based methods and created a binary phage-based system reporter assay for detection of *E. coli*. The mechanism of the method is shown in Figure 1.3. *luxI* incorporated reporter phage (λ_{*luxI}) inserts *luxI* into the *E. coli* XL1-Blue chromosome upon infection. The *luxI* gene is then transcribed, and thereby acyl-homoserine lactone (AHL) autoinducer is produced. The AHL molecules cooperate with the LuxR regulatory protein to stimulate *luxCDABE* transcription in the bioluminescent bioreporter cell λ-phage resistant *E. coli* OHHLux to generate bioluminescence. This method obtained near real-time screening, high specificity, wide detection limits (*E. coli* inoculum range from 130 to 1×10^8 CFU ml^{-1}) and reagentless performance.

1.2 Mycobacteriophages

1.2.1 Introduction to Mycobacteriophage

Mycobacteriophages are mainly isolated by infecting the fast-growing nonpathogenic *M. smegmatis*, and some of them can also infect *M. tuberculosis* as well [25], which makes it possible to prepare phage therapy agents to tuberculosis in a fast and safe
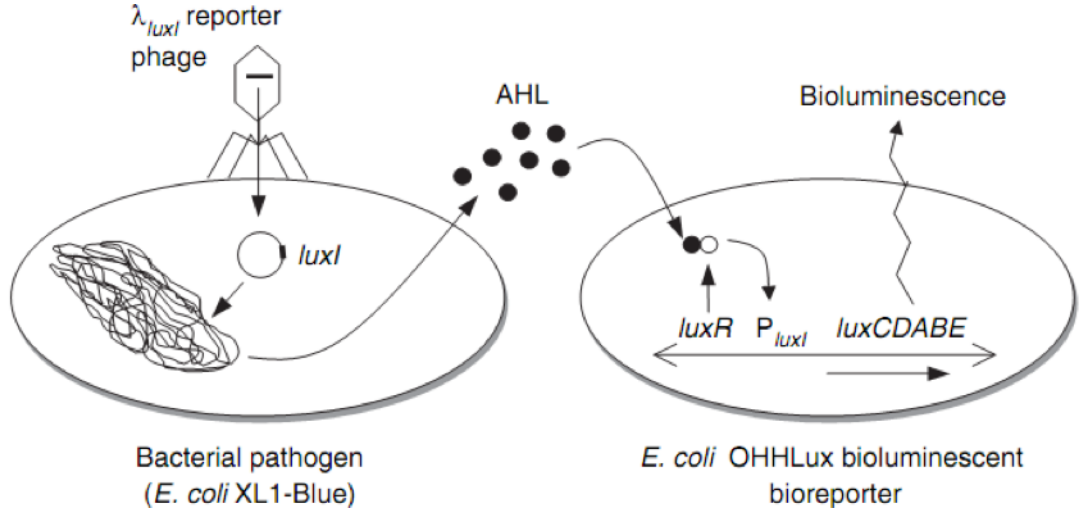
Fig. 1.3. Reporter phage assay for detection of *E. coli* [24].

way. Novel mycobacteriophages are isolated from environmental samples, and phage genomes are sequenced and annotated [26]. Mycobacteriophages can be categorized into clusters through a four-step analysis at the nucleotide level: dot-plot comparison of all genomes with one another, pairwise average nucleotide identities (ANI), pairwise genome map comparisons, and gene content analysis [26]. There are over 10,000 mycobacteriophages belonging to 30 clusters isolated [The Actinobacteriophage Database, 2018]. Functions of annotated gene products are predicted through bioinformatics analysis and homologous proteins are grouped into different phamilies [25].

1.2.2 Mycobacteriophage Genes and Proteins

Every year, genomes of newly isolated mycobacteriophages are annotated using bioinformatics tools including DNA Master and Phage Evidence Collection And Annotation Network (PECAAN). Functions the gene products are annotated by comparing to the proteins in databases including The National Center for Biotechnology Information (NCBI) and HHPred based on the similarities, which provides the basic

understanding of the mycobacteriophage. Mycobacteriophage genomes, which have mosaic structure, usually consists of several basic cassettes: lysis, integration (for temperate phages only), and structural and assembly [25]. Most of the phage proteins are expressed during phage infection inside host bacterial cells, therefore it is very difficult to extract these proteins. Phage particles are coated by the structural proteins, thus, structural proteins such as capsid proteins and tail proteins can be directly extracted from phage lysate. Lysin/holin proteins are well-studied because of the interests in lysis activities. These proteins are usually transfected into a different organism, and the expressed proteins are then extracted and studied. Figure 1.4 shows an example of annotated phage genes and putative gene products.
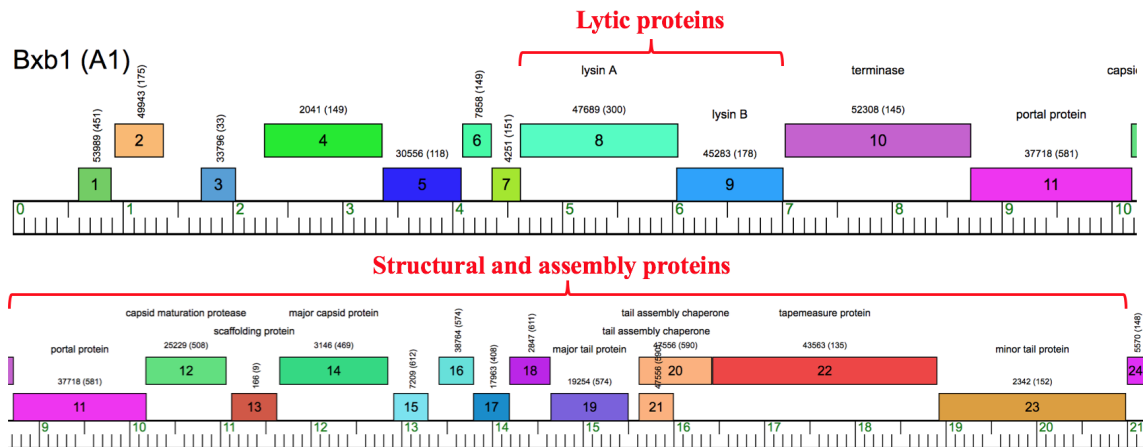
Fig. 1.4. Annotated genes and putative gene products of mycobacteriophage Bxb1 [25].

1.2.3 Mycobacteriophage Lipids

Besides coating proteins and genome, lipids were also found in some mycobacteriophages. Mycobacteriophages D29 [27], DS6A [28], and R1 [29] have been reported to possess lipids. In D29, there are two lipids belonging to none of phospholipids, glycolipids, or peptidolipids [27].

1.3 *M. smegmatis*

1.3.1 Mycobacteria and *M. smegmatis*

Mycobacteria are a genus of actinobacteria, a phylum of Gram-positive bacteria [30]. Mycobacterial cells are rod-shaped with a diameter around 0.3-0.5 μm [31]. As a member of Gram-positive bacteria, mycobacterial envelopes consist of a plasma membrane and a surrounding cell wall [32]. The thick and waxy hydrophobic lipid-rich cell envelope has low permeability, which enables the mycobacterial cell to survive in therapeutic treatment. The significant high content of lipids in the cell wall results in inefficient Gram staining of mycobacteria [33]. Mycobacteria consists of over of 50 species including both pathogenic (*M. tuberculosis* and *M. leprae*) and saprophytic bacteria (*M. smegmatis*) [34, 35]. The phylogenic relationship investigated by using 16S rRNA sequences indicated that Mycobacteria can be divided into fast- and slow-growing subgroups [34]. Mycobacteria usually have long doubling time comparing to the other fast-growing bacteria such as *E. coli*, so the gene regulation systems of mycobacteria must be very different from the fast-growing bacteria [36]. *M. smegmatis* is one of the fast-growing mycobacteria and has a doubling time of about 3-4 hours [36]. Due to fast-growing and possessing orthologues of many *M. tuberculosis* proteins, non-pathogenic *M. smegmatis* has been used as an experimental laboratory model for *M. tuberculosis* [37]. Although the genome of *M. smegmatis* is already sequenced and annotated, functions of lots of the gene products remain unknown.

1.3.2 Mycobacterial Cell Envelope

As shown in Figure 1.5, mycobacterial cell envelope consists of plasma membrane and cell wall [38]. The outer layer of the cell wall is composed of both proteins and polysaccharides [32]. Most of these proteins and polysaccharides are associated with pathogenesis, transportation and intercellular interaction [39]. The inner layer of the cell wall is mainly formed by peptidoglycan (PG), arabinogalactan (AG), and mycolic

acids (MA) which extend from the plasma membrane. The MA-AG-PG complex is the target of many anti-mycobacterial agents [33]. In host cells, mcybacterial cells form a capsule outside of the cell wall [38]. Mycobacterial cell wall is not static, and its structure changes during cell growth and morphogenesis. He and De Bucks research suggests that the proteins in mycobacterial cell envelope may relocate when the physiology of the cells changed [39].
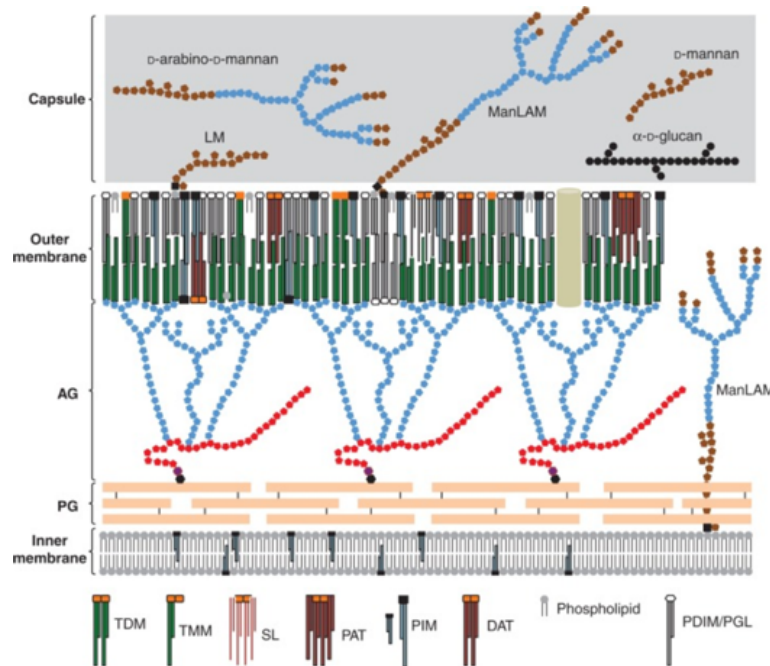
Fig. 1.5. Schematic representation of the M. tuberculosis cell envelope [40].

1.3.3   Lipids in Mycobacterial Cell Envelope

Lipids in mycobacterial cell envelope occupy around 30-60% of the dry cell mass of mycobacterial cell [41]. Different from the major lipid classes which are identified in other organisms, *M. tuberculosis* has some special lipid classes [42]. Forty out of 58 lipid classes identified in *M. tuberculosis* do not have counterparts in other organisms [43]. The main classes of lipids occurring most mycobacteria species include

mycolic acids (MAs), phenolic glycolipids (PGLs), sulfolipids (SLs), tracylglycerols (TAGs) and phthiocerol dimycocerosates (PDIMs) [44].

Mycolic acids (MAs) are long chain fatty acids that are unique in the cell walls of the mycobacteria [45]. MAs are either unbound (free MAs) or covalently linked to AG [46]. In *M. tuberculosis*, three main types of mycolic acids are producted: α-(>70%), methoxy- (10-15%), and keto- (10-15%) [47]. MAs contribute to cell envelope permeability of *M. tuberculosis*, and also involve in biofilm formation [48, 49].

Glycerophospholipids such as phosphatidylethanolamine (PE), phosphatidylinositol (PI), phosphatidylglycerol, phosphatidylserine (PS) and cardiolipin (CL) are the major components of plasma membrane [40]. PE, phosphatidylinositol mannoside (PIM), lipomannan (LM) and mannose-capped lipoarabinomannan (ManLAM) present in the outer layer of mycobacterial cell envelope [40]. Other lipids including trehalose monomycolates (TMMs) and trehalose dimycolates (TDMs), PDIM, SL, diacyltrehaloses (DATs), polyacyltrehaloses (PATs), and PGLs locate in outer membrane or surface of the cell envelope. TDM and TMM are essential for mycobacterial cell envelope [40]. SL, DAT, PAT, PDIM and PGL are involved pathogenicity of mycobacteria [40]. Triglycerides (TAGs) are the intracellular lipids that act as energy reserve in mycobacteria [50, 51].

1.4   Gaps of Current Understanding of Phage-bacteria Interaction

Interactions between the host bacterial cells and the phage are epitomized in either lytic or lysogenic phage life cycles as displayed in Figure 2. However, this model solely focuses on phage, in which the type of phage decides the ability to choose life cycles.

Phages are just virion particles that are unable to replicate and metabolize. Both lytic and lysogenic cycles of phages rely on host cells machinery. Therefore, as the other participator in phage-bacteria interaction, the host bacterial cells may also contribute to the life cycles of phage. Although bacterial cells from the same strain have no genetic variation, individual cells may show distinct responses to lethal stress from

the environment, which ultimately results in survival of a fraction of the cells [52,53]. Such fractional killing occurred in bacterial cells treated by ampicillin, and the survival cells were called persisters [54–56]. The persisters may include some non-dividing cells, as penicillin does not eliminate bacterial cells at stationary phase very efficiently [57,58]. It was also assumed that bacteria might adjust growth rate for better survival in the changing environment [59]. Thus, it is possible that the persisters prefer growing slowly or pause growing [60]. Wakamotos research proved that isoniazid eliminated *M. smegmatis* in different phases: delay, killing and persistence [60]. Similar to the fractional killing of ampicillin, facing to the lethal threat of phage infection, host bacterial cells may be a dynamic population consisting of cells giving different responses to phage infection. Some of the cells may lysed by phage, and some may turn unsusceptible to phage infection.

Since phage infection initiates from the phage attachment to the host bacterial cell, surface and cell wall properties of the host bacterial cells may impact phage-bacteria interaction. One of the major factors that can alter cell surface and cell wall properties is growth phase. In the natural state, bacterial growth is complicated due to the diversity of environmental conditions [61]. Three well-studied non-growth responses of bacteria to environmental stress is: endospore [62], dormancy [63], and viable-but-nonculturable (VBNC) state [64]. *M. tuberculosis* was reported to enter dormant state, which caused insensitive to antibiotics [65]. Thus, it is possible that host bacterial cells in different growth status have different response to phage infection. Since mycobacterial cell envelope consists of both bacteria and abundant lipids, the composition of the envelope proteins and lipids may be associated with surface and cell wall property change in different growth phases (Figure 1.6).

1.5 Objectives of This Research

In this research, the phage-bacteria interaction will be studied in the system of *M. smegmatis* and mycobacteriophages. The research will be conducted in the following
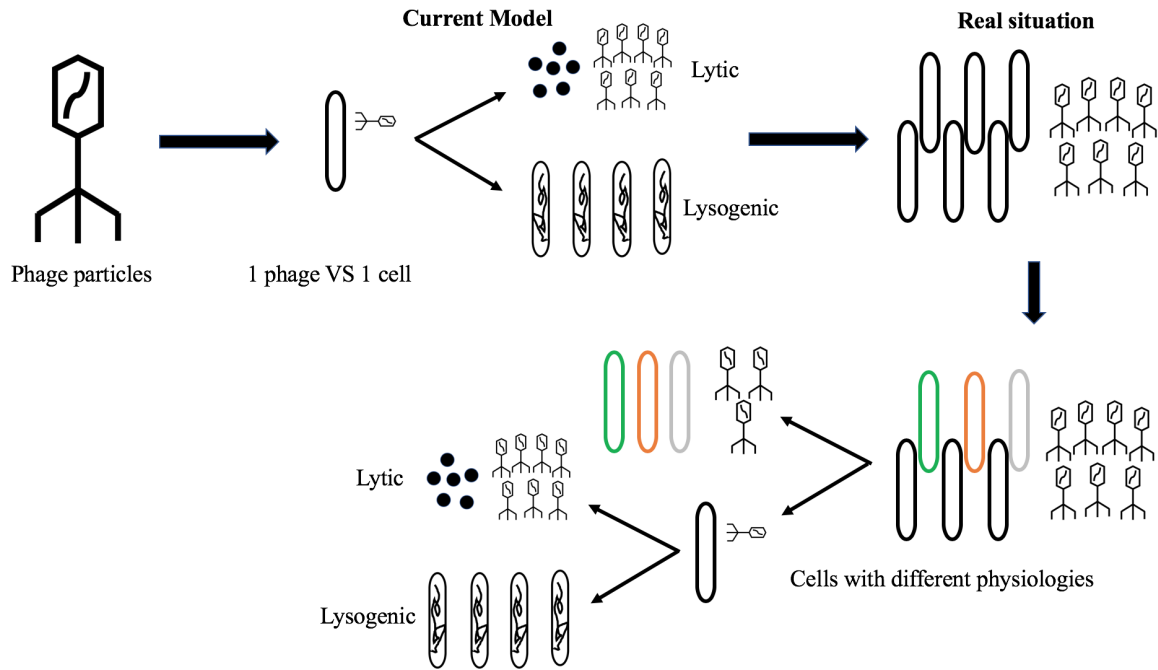
Fig. 1.6. Gaps of current understanding of phage-bacteria interaction. Cells in the same bacterial strain may have different physiologies, which results in different responses to the phage infection.

procedures: (1) Develop a mass spectrometry-based method to study phage proteins in phage-bacteria mixture. (2) Determine the growth curves of the *M. smegmatis* cell cultures at different growth phases infected by different phages, and unveil the impact of bacterial physiology on phage life cycles. (3) Analyze the proteomics of phage-bacteria mixture using mass spectrometry. (4) Analyze the lipidomics of the phage-bacteria mixture using mass spectrometry.

It is expected to update the understanding of phage-bacteria interaction from phage-focusing to a dynamic system dominated by host bacterial cells. The results will also provide experimental evidence to improve the current phage therapy strategies.

2. INVESTIGATE MYCOBACTERIOPHAGE PROTEINS IN PHAGE-HOST MIXTURE BY MASS SPECTROMETRY

2.1 Introduction

In this Chapter, proteomics of 15 mycobacteriophages in phage-host mixture are investigated by mass spectrometry. The results will provide evidence for (1) phage proteins need to be studied in phage-host mixture and (2) the mass spectrometry results validate of phage genome annotation.

2.2 Materials and Methods

2.2.1 Phage stocks

Stocks of fifteen phages (Table A.1) were obtained from Prof. Graham Hatfulls research group through the Howard Hughes Medical Institute (HHMI) Science Education Alliance-Phages Hunters Advancing Genomics and Evolutionary Science (SEA-PHAGES) program

2.2.2 Protein Extraction

A portion of *M. smegmatis* 48-hour culture (5 ml) and 100 mul of phage stocks were incubated together in a 250 ml sterile Erlenmeyer flask overnight at 37°C with shaking. After the incubation, the phage-bacteria mixture was transferred into a 15 ml conical tube and centrifuged for 10 minutes at 1,000×g. The pellet was collected and resuspended with 100 μl of 100 mM ammonium bicarbonate. A PCT microtube containing 100 μl of the mixture was placed in Barocycler NEP 2320 (Pressure Bio-

Sciences Inc.) for cell lysis at 35,000 psi for 30 to 80 cycles at room temperature. Protein concentration of each sample was estimated using nitrocellulose paper and Bradford assay. A portion (50 μl) of each sample from the barocycler was transferred into a 1.5 ml microcentrifuge tubes. The samples were mixed with 100 μl of chloroform/methanol (2:1) and centrifuged for five minutes at maximum speed. The lower phase of the sample was discarded and sterile water was added to bring the total volume up to 100 μl. Four times the volume of -20°C acetone was added to the sample. The sample was mixed by vortex and centrifuged for 5 minutes at maximum speed. The supernatant was removed and the pellet was saved. The protein pellet was resuspended with 10 μl of denaturation solution (8 M urea + 10 mM dithiothreitol in 10 ml water). This solution was incubated at 37°C for 0.5 to 1.5 hours. After that, 10 μl of freshly prepared cocktail (195 μl of acetonitrile, 1 μl triethylphosphine, and 4 μl 2-iodoethanol) was added to the sample and incubated at 37°C for 0.5 to 1.5 hours. The sample was then completely dried by speed vacuum.

2.2.3   Mass Spectrometry

Trypsin was added (1 μg trypsin per 50 μg protein) to digest the dry sample at 37°C for at least 12 hours. Digestion was stopped by adding 1 μl of 10% trifluoroacetic acid (TFA). Finally, 20 μl of 0.01% TFA was added to the sample to bring final concentration to 1 μg/μl. Protein concentration was estimated using nitrocellulose paper. The trypsin-digested proteins were then separated by High Performance Liquid Chromatography (HPLC) and introduced into a mass spectrometer for fragmentation and sequencing to identify the parent proteins. The tryptic peptides were separated on a nanoLC system (1100 Series LC , Agilent Technologies, Santa Clara, CA). The peptides were loaded on the Agilent 300SB-C18 enrichment column for concentration and the enrichment column was switched into the nano-flow path after 5 minutes. Peptides were separated with the C18 reversed phase ZORBAX 300SB-C18 analytical column (0.75 μm×150 mm, 3.5 μm) from Agilent. The column was con-

nected to the emission tip from New Objective and coupled to the nano-electrospray ionization (ESI) source of the high resolution hybrid ion trap mass spectrometer LTQ-Orbitrap XL (Thermo Scientific). The peptides were eluted from the column using an acetonitrile (ACN)/0.1% formic acid (FA, mobile phase B) linear gradient. For the first 5 minutes, the column was equilibrated with 95% H_2O/0.1% formic acid (mobile phase A) followed by the linear gradient of 5% B to 40% B in 45 minutes at 0.3 μl/min, then from 40% B to 100% B in additional 5 minutes. The column was washed with 100% ACN/0.1% FA and equilibrated with 95% H_2O/0.1% FA before the next sample was injected. A blank injection was run between samples to avoid carryover. The LTQ-Orbitrap mass spectrometer was operated in the data-dependent positive acquisition mode in which each full MS scan (30.000 resolving power) was followed by eight MS/MS scans where the eight most abundant molecular ions were selected and fragmented by collision induced dissociation (CID) using a normalized collision energy of 35%.

2.2.4 Investigate the Impact of Software and Databases

The raw files from the mass spectrometer were converted using msconvert ProteoWizard [66] to the mgf format and submitted to database search using the software X! Tandem (www.thegpm.org/tandem) and Mascot (www.matrixscience.com). Two databases were created: (1) The proteins available on UniProt (08/17/2018) for each phage and the annotated proteins of *M. smegmatis* (UniProt 08/17/2018); (2) The six-frame translation of the phage genome (PhageDB 08/17/2018) and the annotated proteins of *M. smegmatis* (UniProt 08/17/2018). The six-frame translation of phage genomic DNA sequences were obtained using Transeq from EMBOSS Tools [67] and the protein sequence smaller than seven amino acid was removed. The output files from X! Tandem and Mascot software were analyzed by X!TandemPipeline 3.4.1 software (pappso.inra.fr). The raw data was searched against the two database in X!

Tandem and Mascot, and the total numbers of peptides identified were collected and compared.

2.2.5 Phage Protein Identification Using X! Tandem

The mgf format of raw data from the orbitrap instrument was processed using X! Tandem and searched against the database comprised of the six-frame translation of the phage genome and the annotated proteins of *M. smegmatis* (UniProt 08/17/2018). The phage peptides identified were first looked up in the annotated phage proteins. The remaining phage peptides that could not be found in any annotate phage proteins were then marked in the six reading frames of their own genome in Artemis (Trust Sanger Institute).

2.3 Results

2.3.1 Sample Preparation

The overall experimental process is shown in Figure 2.1. Individual phage stocks were incubated separately with *M. smegmatis* cell culture and provided maximum time for infection and production of phage proteins by the infected bacteria. Non-infected *M. smegmatis* cell culture was used as a negative control. Proteins from the phage-bacteria mixture were extracted using high pressure to break the cell membrane, digested with a protease enzyme and loaded to mass spectrometer for analysis.

2.3.2 Impact of Software and Databases on Peptides Identification

Two software (Mascot and X! Tandem) and two distinct databases were empolyed to study the impact of software and database on peptide identification. X! Tandem is open source, free for academic project and was used in other mycobacteriophage researches [68,69]. Mascot, developed by Matrix Science Inc., is often used in Bindley Bioscience Center, Purdue University. The two distinct databases are (1) combination
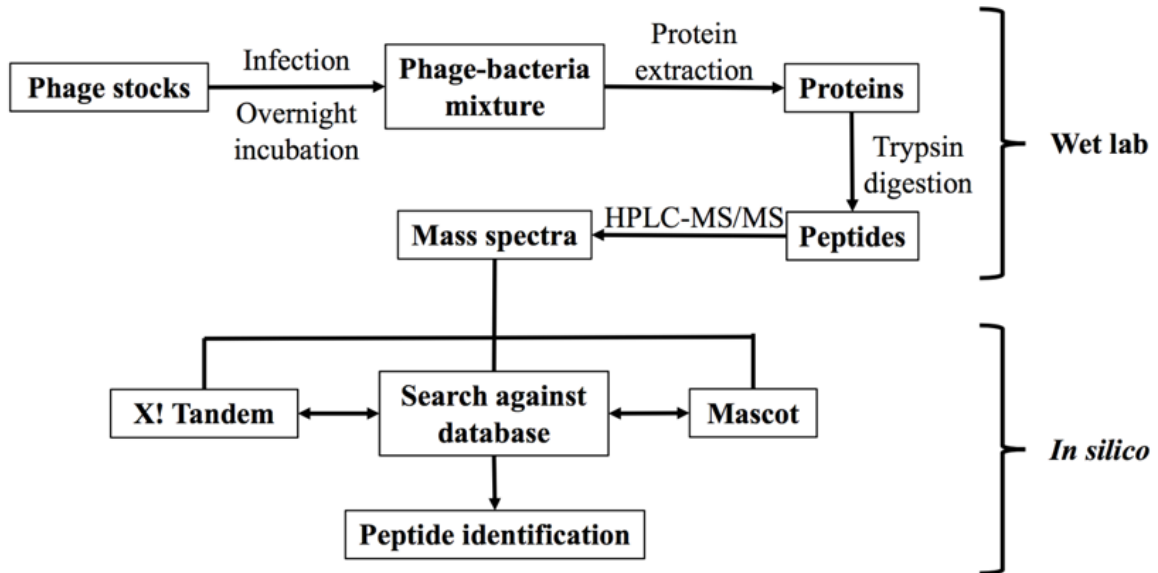
Fig. 2.1. Flowchat of the experiment.

of annotated proteins of the sample phage and annotated proteins of *M. smegmatis*; (2) combination of six-frame translation of the sample phage genome and the annotated proteins of *M. smegmatis*.

The use of different software and databases resulted in a variable number of identified peptides (Figure 2.2). X! Tandem and Mascot identified similar amount of phage peptides. X! Tandem identified about 27% more peptides of LinStu than Mascot did. When using X! Tandem, , in Kugel and Avrafan, the database consisting phage six frame translation and *M. smegmatis* annotated proteins identified none phage peptides, while the other database identified 90. As previous research mentioned that out-of-frame peptides which were not included in the annotated proteins were expressed in phage samples [68], six frame translation of phage genome may help identify the out-of-frame peptides. Therefore, X! Tandem and the database of six-frame translation of the sample phage genome and the annotated proteins of *M. smegmatis* is the appropriated tool to study phage proteins in phage-host mixture.

Number of phage peptides identified
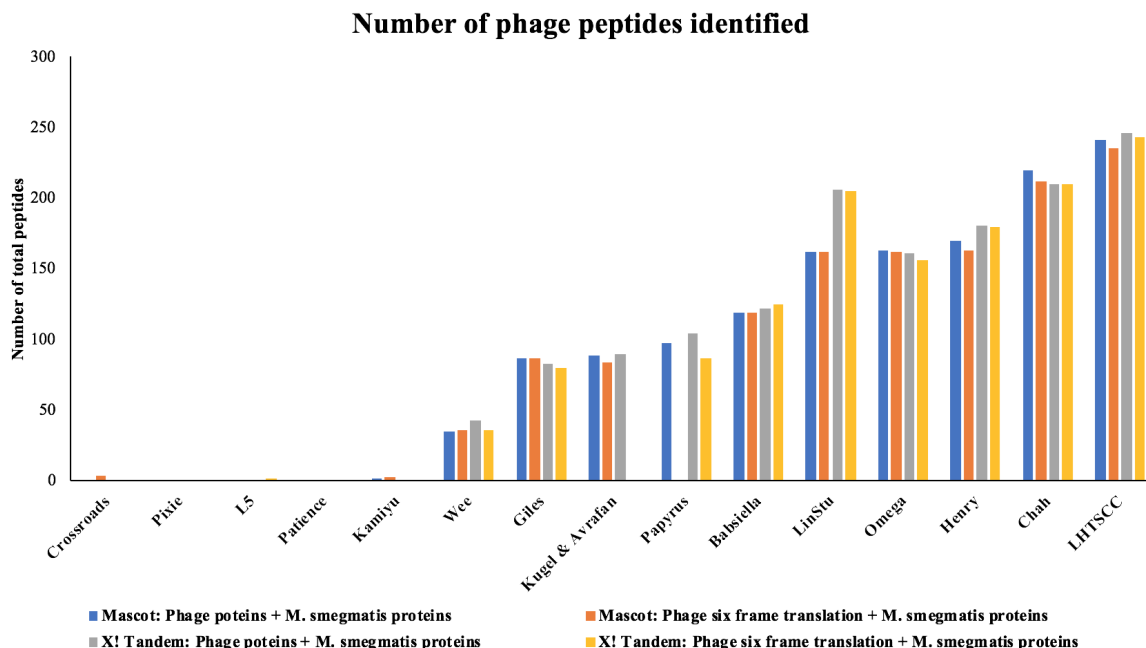
Fig. 2.2. Number of phage peptides identified in all sample phages using Mascot and X! Tandem and two distinct databases. Mass spectra data was searched against four distinct databases using Mascot and X! Tandem. Databases were: (1) Annotated proteins the sample phage and the annotated proteins of *M. smegmatis*; (2) six-frame translation of the genome of the sample phage and the annotated proteins of *M. smegmatis*.

2.3.3   Phage Protein Identification Using X! Tandem

The phage peptides identified with X! Tandem were labeled in the genome map of the phages to compare the expressed phage proteins with the putative proteins from the phage genome annotation. Only one protein was identified in Kamiyu, and seven proteins were identified in Wee. More than 30 proteins were identified in Chah, LinStu and Omega. Although only portion of the putative proteins predicted from the genome annotations were identified, the detected peptides validated the existing genome annotations for the corresponding genes. As expected, putative virion structure and assembly proteins were detected in all samples, suggesting the presence

and production of phage virions. Non-structural proteins predicted by the genome annotations were also detected as described in the following paragraphs.

There were 18 proteins detected in Babsiella (Table A.2), including LysA and LysB (proteins that promote host cell lysis), structure and assembly proteins, FtsK domain protein and DNA methylase domain protein. Che9c is a well-annotated member of Cluster I. The first 22 genes from Che9c are virion structure and assembly proteins [25]. Based upon a comparison to Babsiella using Phamerator [70], the first 22 putative proteins of Babsiella have a similar structure and distribution and belong to conserved phamilies (Figure 2.3). Therefore, although gp5 (gene product of gene 5), gp8, gp13 and gp21 of Babsiella are functionally uncharacterized, their putative proteins may be associated with virion structure and assembly based upon comparison in Phamerator which is a software that is used for comparative genomic analysis and characterization of phamilies [70]. The remaining proteins identified, gp75 and gp76, have unknown functions.
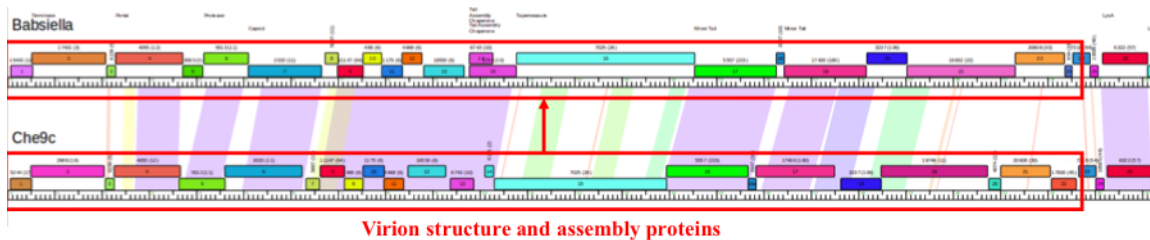
Fig. 2.3. Comparison between the genomes of Babsiella and Che9c. The genomes of Babsiella and Che9c were compared using Phamerator [70]. Most of the first 22 genes in both genomes belong to the same phamilies (same color and phamily number) and have similar distribution.

A peptide in upstream of gp76 and overlapping with gp75 was found in the sample (Figure 2.4). Since the annotation gene 76 was only accomplished in silico, the detected of this upstream peptide of gp76 may indicate an extended gene 76.

Fig. 2.4. An upstream peptide of gp76 in Babsiella was detected.

There were 38 proteins were detected from Chah (Table A.3), a phage from Sub-cluster B1. Among the detected proteins, only eight had putative functions assigned based on genome annotation efforts. Potential functions include proteins responsible for: virion structure and assembly such as portal (gp9), capsid (gp12), major tail subunit (gp18) and tapemeasure protein (gp29); host cell lysis such as LysA (gp50) and LysB (gp51); and DNA replication such as helicase type III restriction subunit (gp54) and RepA helicase (gp60). An upstream peptide covering 42 amino acids of gp74 was detected (Figure 2.5), which suggested an extended gene 74.

Fig. 2.5. An upstream peptide covering 42 amino acides of gp74 in Chah was detected.

There were 18 proteins detected from Giles (Table A.4), one of the 12 phages from Cluster Q. Six of the 18 proteins detected are putative virion structure and assembly proteins. In addition, protease (gp7), a protein involved in a protease-required capsid assembly process [25], and Lysin A and B (gp31 and gp32) were also detected along with functionally uncharacterized proteins, gp3, gp8, gp15, gp18, 37, gp58, gp59 and gp60.

Two out-of-frame peptides were detected in Giles. One of them was in upstream of gp38 (Figure 2.6(a)). It may indicate the existence of a putative gene in this area. The other peptide was in upstream of gp18 and had two amino acids overlap with gp18 (Figure 2.6(b)). It suggested that the actually gp18 was longer than the annotated gene product.
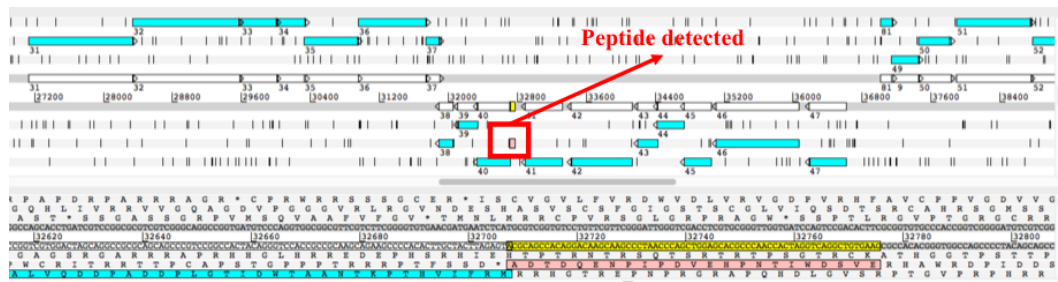
(a) Peptide in upstream of gp38
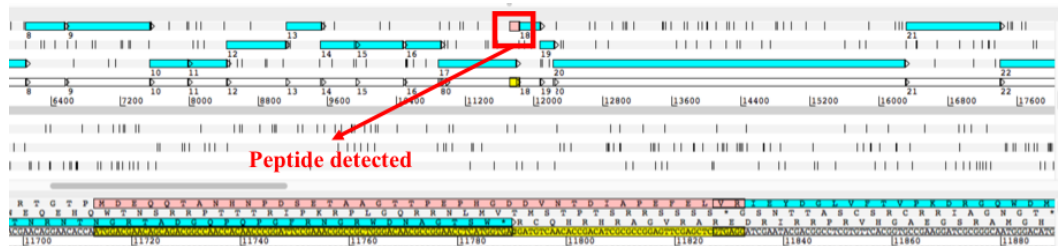
(b) Peptide overlap with gp18

Fig. 2.6. Out-of-frame peptides detected in Giles.

There were 28 proteins detected from the phage sample, Henry (Table A.5), a member of Cluster E. Putative proteins for virion structure and assembly, lysis and DNA replication were detected, similar to results from the phage sample, Chah. The

rest proteins detected were not functionally characterized based upon the genome annotation. Performing a genome homology analysis with Phamerator, however, suggests that gp34 from Henry is a holin, based upon homology with the holin (gp33) of another phage from Cluster E, Cjw1 (Figure 2.7).
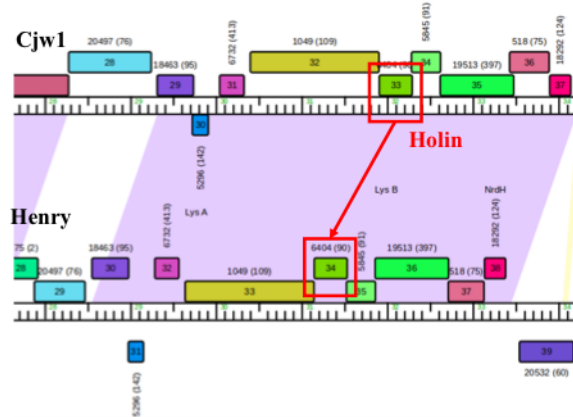
Fig. 2.7. Comparison between the genomes of Henry and Cjw1. The comparison was obtained by using Phamerator. Gp34 of Henry and gp33 of Cjw1 have an E-value of 0.0 and are from the same phamily. Therefore, gp34 of Henry may also be a putative holin protein based upon homology with the putative holin protein (gp33) of Cjw1.

Similar to observations in other phage samples, there were 27 proteins detected from LHTSCC (Table A.6), a Cluster A4 phage, again including those with putative functions in virion structure and assembly, lysis and DNA replication. Unique proteins not detected in other phage samples were also observed, including a putative recombination directionality factor (RDF) and thymidylate synthase. As shown in Figure 2.8, there were two out-of-frame peptides were detected which indicated that the actual gp14 and gp26 were longer than the annotated ones.

Similar to other phage samples, most of the peptides detected in the remaining phage samples LinStu (Cluster C1, Table A.7), Omega (Cluster J, Table A.8), Papyrus (Cluster R, Table A.9), and Wee (Cluster F1, Table A.10), were virion structure and assembly proteins. Other proteins involved in DNA replication and lysis were also detected in the phage Omega. The functions for the remaining proteins detected
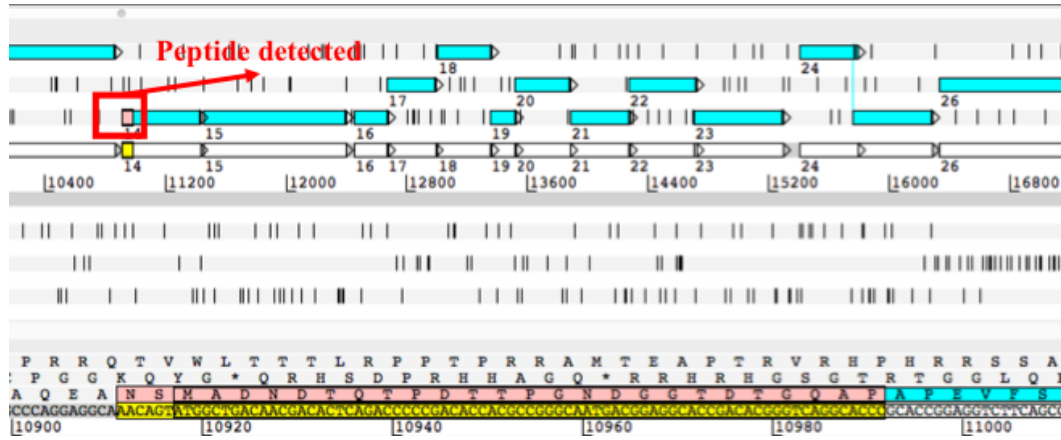
(a) A peptide of LHTSCC scaffold protein (gp14) covering 25 amino acids upstream from the annotated start site.

(b) A peptide of LHTSCC tapemeasure protein (gp26) covering 11 amino acids upstream from the annotated start site.

Fig. 2.8. Out-of-frame peptides detected in LHTSCC.

were not characterized, as in the phage Papyrus where the putative functions of 15 of the 21 proteins detected in the phage sample were unknown. Kamiyu only had one peptide of gp11 with unknown function detected. L5 had out-of-frame peptide in the gap between gp32 and gp34, which may indicate that the reverse gene 33 should be forward (Figure 2.9).
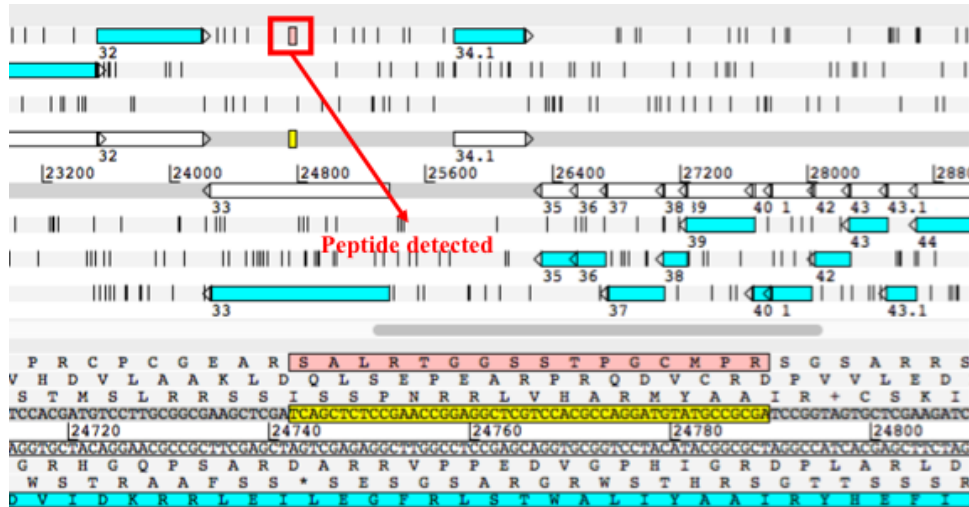
Fig. 2.9. An out-of-frame peptide was detected in L5

In summary, the use of X! Tandem and the database consisting of six frame translation of phage genome and *M. smegmatis* annotated proteins proved to be a quick way to validate annotated proteins.

2.4 Discussions

2.4.1 Impact of software and database

Software analysis and database selection is critical in this research. An optimized combination of software and database can identify and quantify both phage and bacterial proteins in the same profile, which saves enormous effort on separating phage proteins from bacterial proteins and also provides an effective way to study both phage proteome and bacterial proteome in the phage-bacteria mixture. In the future, this method may be modified to study the proteome of individual organisms over time in other complex systems.

In this research two software and two databases were compared. The results demonstrated that X! Tandem and the database consisting of phage genome six frame translation and *M. smegmatis* annotated proteins is the optimal tool to identify pep-

tides detected in mass spectrometry. It also found out-of-frame peptides that could improve phage protein annotation.

2.4.2 Studying Phage Proteins and Life Cycles in A Dynamic Phage-host system

The method designed in this research provides an effective way to study uncharacterized phage proteins through native expression in the phage-host dynamic system. Previous studies used recombinant protein expression to characterize the function of non-structural proteins [71–73]. The recombinant expressed proteins, however, may differ from the native phage protein and this could impact function. Native phage proteins may undergo unique posttranslational modifications including the addition or removal of specific amino acid residues [74–76]. Since phage proteins perform specialized functions in host bacterial cells, it is likely that native phage proteins have certain properties that facilitate functional interactions with host bacterial proteins. In fact, recent research [77] revealed that the protein encoded by lysin A of phage D29, is only active in *M. smegmatis* and becomes inactive in *E. coli*.

The mechanism of the phage protein expression is not well understood. Since the phages do not have native metabolism, the phage protein expression relies on the hosts machinery. When the physiology of the host changes, the pattern of protein expression for the phage is also likely to change in response.

Previous research showed that wildtype *E. coli* cells, infected with a single phage, or with multiplicity of infection (MOI) of one, will predominantly be lysed; if MOI is higher than two, the lysogenic cycle is preferred over the lytic cycle [78, 79]. It was reported that the frequency of the lysogenic cycle would be increased in an environment that was not favorable for bacterial proliferation [80].

The studies above suggest that both *M. smegmatis* cell culture growth phases and MOI affect the phage life cycle. In order to obtain a high frequency of the phage lysogenic cycle, St-Pierre and Endy grew *E. coli* cell culture for phage infection to

stationary phase [81]. Pope *et al.* investigated protein expression of the mycobacte-riophage Patience by infecting exponentially growing *M. smegmatis*, and found that the peptide amount of some proteins changed within the first 2.5 hours after infection [68].

Future studies investigating changes in phage protein expression isolated from infected bacterial cells over time, could provide a better understanding of the putative phage proteins beyond previous methods focusing solely on purified phage virion particles. A better understanding of the phage protein expression pattern could help expand the applications of phage. Diverse applications could include: a phage-based biosystem with deterministic behavior based on the mechanism of lytic-lysogenic life-cycle alteration, production of anti-bacterial phage agents with higher efficiency, and creation of new functional cassettes and modules (BioBricks) for synthetic biology as novel phage proteins are characterized.

2.4.3   Limitation of this research

Most of the peptides detected from the mass spectrometry experimental analysis, validated the existing phage genome annotations of putative proteins. A more thorough validation was limited, however, by the number of peptides detected and the overall coverage of the translated genomic sequence. The matching peptides did not overlap with annotated start sites for putative proteins with some notable exception: the peptides from Babsiella, Chah, Giles, and LHTSCC that matched locate in up-stream predicted annotated start site. These peptides suggest that the actual start site of the proteins may be different from the current annotated start site. In future experiments, we will explore strategies to optimize coverage and the number of phage peptides isolated and subsequently detected and analyzed, by changing variables such as the titer of phage, the incubation time before sample isolation, and the mixture of protease used to digest the isolated proteins prior to mass spectrometry.

2.5 Conclusions

In this research, we developed a mass spectrometry-based method that can investigate phage proteins in phage-bacteria mixture, and tested the impact of different software and databases on peptide identification. The results substantiated the importance of appropriate software and database, and highlighted that the method provided an effective way to study native phage proteins in a dynamic phage-host system. In the future, the method will be improved to increase the amount of phage peptides and optimize the phage peptide identification.

3. GENOME ANNOTATION OF 19 MYCOBACTERIOPHAGES ISOLATED AT PURDUE UNIVERSITY

There are 151 phages isolated at Purdue University from 2010 to 2017 (105 obtained in and after 2013). Genomes of 22 phages were sequenced and annotated in total (19 done in and after 2013) (Table 3.1). Half of the annotated phages belong to Cluster A. The other half included the phages from Clusters B, C, E, F, J, O and S.

Table 3.1.
The 19 phages annotated after 2013

Phage	Cluster	Genome (bp)	GC%	Gene	tRNA	tmRNA	GenBank Accession
AFIS	A1	51737	63.7	90			Under review
Cosmolli16	B1	68978	66.5	103			Under review
Czyszczon1	E	75075	62.9	141	2		Under review
EricMillard	J	113536	60.9	252	1		MH697583
Fibonacci	A11	52462	63.8	99	1		Under review
FrenchFry	B2	67494	68.9	95			MH697584
Grand2040	B1	68591	66.4	101			MH744417
Hughesyang	J	112884	60.9	254	1		Under review
JewelBug	A6	50341	61.6	98	3		Under review
Lemur	A4	51370	63.9	91			Under review
Mesh1	B1	68774	66.4	103			MH825705
MilleniumForce	F1	58106	61.8	116			MH825707
Ochi17	F1	58069	61	124	3		Under review
Pept2012	A1	51703	63.7	89	1		Under review
PotatoSplit	A3	50886	64	94	4		Under review
Sophia	B1	68306	66.5	103			Under review
VasuNzinga	S	64911	63.4	116			MH727562
Waterdiva	B1	68866	66.5	104			MH779516
Zalkecks	C1	154764	64.7	230	37	1	MH825713

All the phages in Table 3.1 except Waterdiva were isolated from the soil. Waterdiva was obtained from a water sample. Isolation, purification and amplification of the phages were accomplished following the protocols in Phage Discovery Guide from HHMI. High titer lysates (titer $> 5 \times 10^9$ pfu/ml) of the phages were obtained by infecting *M. smegmatis* mc^{2}155 cell culture. Morphology of the phages were observed using transmission electron microscopy (TEM). Genomic DNA of the phages were extracted from the high titer lysates and sequenced by Pittsburgh Bacteriophage Institute by using Illumina Sequencing. The genomic DNA of the phages were subsequently annotated following SEA-PHAGES Bioinformatics Guide. The genome annotation was performed by comparing putative genes and gene products with the well-annotated genes and gene products in databases using tools including DNA Master, Phamerator, HHPred, PECAAN, and NCBI. The annotated genomes of all the phages were submitted to GenBank. The complete genome and annotation information of EricMillard, FrenchFry, Grand2040, Mesh1, MilleniumForce, VasuNzinga, Watediva and Zalkecks are available on GenBank.

Zalkecks has a morphology of myoviridae, and the rest phages in Table 3.1 are all siphoviridae.

As shown in Figure 3.1, Zalkecks (C1) has the longest genome size that is over 154 kbp. EricMillard (J) and Hughesyang (J) also have genomes over 100 kbp. Cluster A phages in Table 1 possess the shortest genomes. AFIS (A1), Fibonacci (A2), JewelBug (A6), Lemur (A4), Petp2012 (A1), PotatoSplit (A3) all have the genomes size just over 50 kbp. Genomes of Cluster B phages, Cosmolli16 (B1), FrenchFry (B2), Grand2040 (B1), Mesh1 (B1), Sophia (B1) and Waterdiva (B1) are all around 67-69 kbp. MilleniumForce and Ochi17, both from Cluster F1, have a genome around 58 kbp. Genomes of Czyszczon1 (E) and VasuNzinga (S) are about 75 kbp and 65 kbp respectively.

As shown in Figure 3.2, GC content of *M. smegmatis* mc^{2}155 is 67.4%. Cluster B phages in Table 1 have the highest GC contents that are all above 66%. GC content of FrenchFry (B2) is 68.9% which is even higher than the GC content of *M. smegmatis*
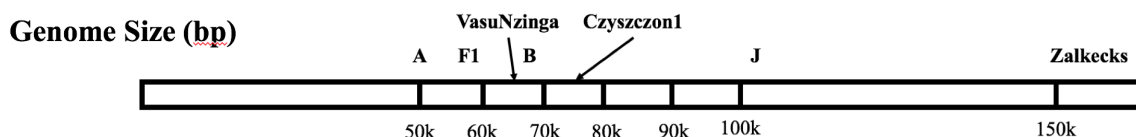
Genome Size (bp)

Fig. 3.1. Genome sizes of the phages.

mc^{2}155. The lowest GC content in Table 1 is 60.9% that is from Cluster J phages EricMillard and Hughesyang.
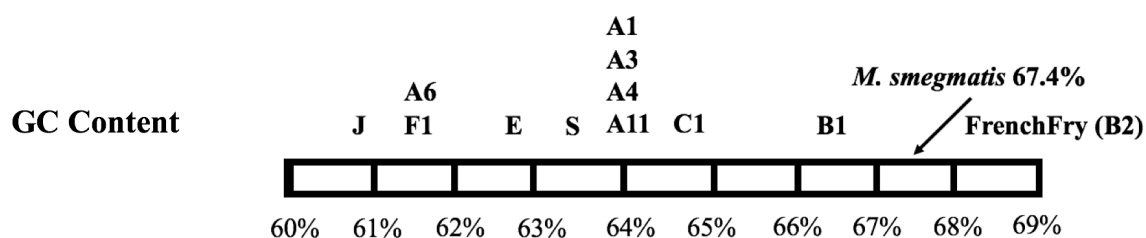
GC Content

Fig. 3.2. GC content of the phage genomes.

In general, the phages all have structure and assembly proteins, lysis proteins, terminase, integration proteins (for temperate phages), and DNA replication proteins. Besides the common proteins, each phage also has some special proteins. AFIS has transpoase, immunity repressor and recombination directionality factor. Cosmolli16 has adenylate kinase, queuine tRNA-ribosyltransferases and recombination directionality factor. Czyszczon1 has NrdH-like glutaredoxin, Lsr2-like DNA bridging protein, polynucleotide kinase, RNA ligase, WhiB family transcription factor, RecA-like DNA recombinase, Clp-like protease and hydrolase. EricMillard has glycosyltransferases, methyltransferases, NrdH-like glutaredoxin, Lsr2-like DNA bridging protein, polynucleotide kinase, serine/threonine kinase, WhiB family transcription factor, MazG nucleotide pyrophosphohydrolase, metallophosphoesterase, LipC-like lipase and FtsK-like DNA translocase. Fibonacci has VIP2-like toxin, Thyx-like thymidylate synthase and immunity repressor. FrenchFry has QueC/QueD/QueE-like queosine biosynthesis

proteins, queuine tRNA-ribosyltransferase, GTP cyclohydrolase I and HicA-like toxin in toxin/antitoxin system. Grand2040 has queuine tRNA-ribosyltransferases. Hughesyang has glycosyltransferases, methyltransferases, galactosyltransferase, NrdH-like glutaredoxin, Lsr2-like DNA bridging protein, polynucleotide kinase, serine/threonine kinase, WhiB family transcription factor, MazG nucleotide pyrophosphohydrolase, metallophosphoesterase, LipC-like lipase, RuvC-like resolvase and FtsK-like DNA translocase. JewelBug has peptidase, deoxycytidylate deaminase, ThyX-like thymidylate synthase, ribonucleotide reductase, metallophosphoesterase, and antirepressor. Lemur has deoxycytidylate deaminase, ThyX-like thymidylate synthase, ribonucleotide reductase, metallophosphoesterase, hydrolase, phosphoribosyl transferase, immunity repressor and SprT-like protease. Mesh1 has RuvC-like resolvase, queuine tRNA-ribosyltransferase and recombination directionality factors. MilleniumForce has immunity repressor, Cro, WhiB family transcription factor, glycosyltransferases and serine/threonine kinase. Ochi17 has immunity repressor, Cro, antirepressor, WhiB family transcription factors, AAA-ATPase, mycobacteriophage mobile element 2 (MPME2), glycosyltransferases and galactosyltransferase. Petp2012 has recombination directionality factor and NrdH-like glutaredoxin. PotatoSplit has deoxycytidylate deaminase, ThyX-like thymidylate synthase, ribonucleotide reductase, recombination directionality factor, esterase and immunity repressor. Sophia has RuvC-like resolvase and queuine tRNA-ribosyltransferase. VasuNzinga has O-methyltransferase, glutamine amidotransferase, glycosyltransferase and galactosyltransferase. Waterdiva has RuvC-like resolvase and queuine tRNA-ribosyltransferase. Zalkecks has nucleotidyl transferase, ThyX-like thymidylate synthase, phosphoesterase, LysM-like endolysin, peptidyl tRNA hydrolase, aminotransferase, DnaJ-like chaperonin, RF-1 peptide chain release factor, polynucleotide kinase, serine/threonine kinase and PurA-like adenylosuccinate synthetase.

Czyszczon1, EricMillard, Fibonacci, Hughesyang, JewelBug, Ochi17, Pept2012, PotatoSplit, and Zalkecks all have tRNAs. Zalkecks has 37 tRNA and 1 tmRNA.

4. PROTEOMICS STUDY OF THE IMPACT OF MYCOBACTERIAL PHYSIOLOGY ON MYCOBACTERIOPHAGE LIFE CYCLE

4.1 Introduction

In this chapter, five of the mycobacteriophages introduced in Chapter 3 are selected to infect *M. smegmatis* cells at both exponential and stationary phases. Proteins will be isolated from the phage-bacteria mixtures and analyzed using mass spectrometry. Correlations between each protein and the experimental factors will be investigated by developing linear regression models. The result will unveil (1) the impact the growth phases of *M. smegmatis* on mycobacteriophage life cycles and (2) the proteins of *M. smegmatis* involved in physiology change.

4.2 Materials and Methods

4.2.1 Growing *M. smegmatis* cell culture

M. smegmatis cell culture from -80°C stock was recovered by streak plating on an LB agar plate. The plate was incubated at 37°C for 72 hours. Then a single colony was inoculated in 7H9 Complete with 0.05% Tween®80 and incubated at 37°C with shaking at 250 rpm for 48 hours. The culture was called Passage 1 From the Frozen (P1FF) stock. Then a small volume of P1FF stock was added to 7H9 Complete (P1FF:7H9 Complete = 1: 10000) and incubated at 37°C with shaking at 250 rpm for 48 hours. The culture was called P2FF, which was used for preparation of mycobacteriophage lysates.

4.2.2 Determine Growth Curve of *M. smegmatis*

OD_{600} of a *M. smegmatis* P2FF culture was determined every 8 hours in the first 122 hours and every 24 hours after. Then the OD_{600} values were plotted and the growth curve of *M. smegmatis* was drawn.

4.2.3 Preparation of Mycobacteriophage Lysates

Five phages (Table 4.1) isolated at Purdue University were selected to infect *M. smegmatis* cell culture. Serial dilutions of the phage lysates from -80°C stocks were prepared using phage buffer. 10 μl of each dilution was mixed with 250 μl of *M. smegmatis* P2FF culture and left on the bench for 10 minutes. Then the mixture was mixed with top agar and poured on to a LB agar plate. The plate was then incubated at 37°C for 48 hours. The webbed plate was selected and soaked by 5 ml of phage buffer to collect the phage particles. The phage lysate was then filtered by a 0.22 μm filter.

Table 4.1.
Five phages from diverse clusters selected for infecting *M. smegmatis* cell culture

	Cluster	GC content (%)	Integrase (Y/N)	Type
Cosmolli16	B1	66.5	N	Lytic
FrenchFry	B2	68.9	N	Lytic
Hughesyang	J	60.9	N	Lytic
JewelBug	A6	61.6	Y	Temperate
MrGordo	A1	63.8	Y	Temperate

4.2.4 Determination of Phage Infection Dynamics

The growth curve of *M. smegmatis* was determined, and OD_{600} of around 0.4 and 3.7 were chosen as the indicators of exponential and stationary growth phases. As

shown in Figure 4.1, a P1FF stock was added to 7H9 Complete (P1FF:7H9 Complete $= 1: 10000$) and incubated at 37°C till stationary phase and subsamples were prepared at OD_{600} of around 0.4 and 3.7. The phage lysate was added into each cell culture subsample with a MOI of 10 and incubated for 10 hours. MOI for JewelBug was 1. OD_{600} of the phage-bacteria mixture was determined over time and plotted to obtain the growth curve. The initial OD_{600} values of all the growth curves of the exponential *M. smegmatis* cell cultures infected by the phages were normalized to 0.4, and the ones of the stationary *M. smegmatis* cell cultures infected by the phages were normalized to 3.7. After 4 and 10 hours of phage infection, 1 ml of the mixture was harvested for total protein extraction, and another 1 ml of the mixture was filtered by a 0.22 μm filter. The titer of the phage in the filtered mixture was determined by serial dilutions and plaque assay. The whole procedures were performed three times to obtain biological triplicates.
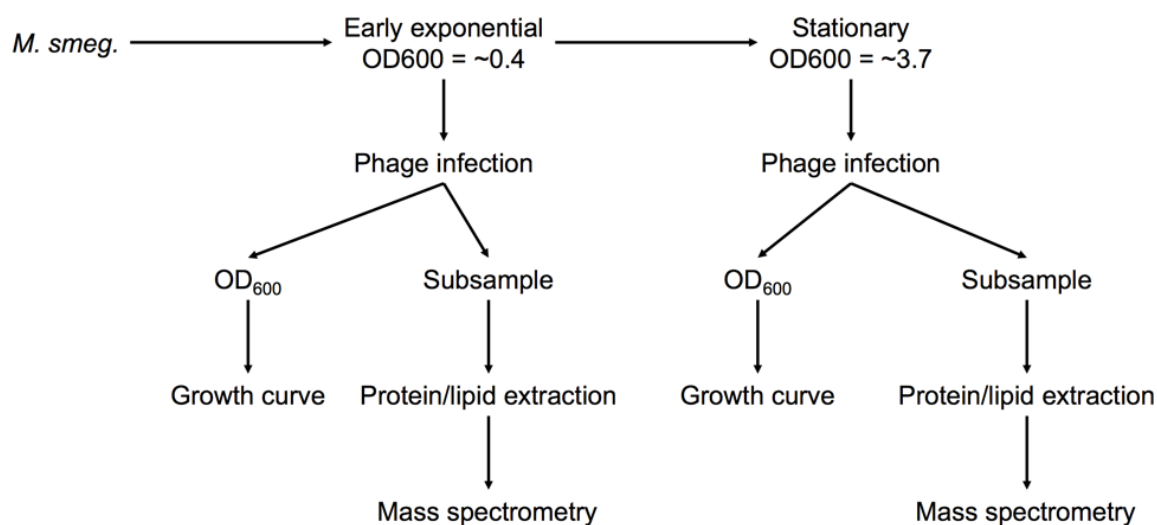
Fig. 4.1. Flowchart of the experiment.

4.2.5   Protein Extraction

The 1ml phage-bacteria mixture was centrifuged at 13,000 rpm for 10 minutes. The pellet was collected and resuspended with 100 μl of 100 mM ammonium bicarbonate. A PCT microtube containing 100 μl of the mixture was placed in Barocycler NEP 2320 (Pressure BioSciences Inc.) for cell lysis at 35,000 psi for 90 cycles at 4°C. Then the sample was transferred to a new microcentrifuge tube and homogenized with double distilled water to 200 μl. The sample was mixed with 250 μl of chloroform and 450 μl of methanol. After vortex, the sample was mixed with another 250 μl of chloroform and 250 μl of double distilled water. Then sample was centrifuged at 6,000 rpm, and three phases were collected separately. The upper phase (metabolites) and the bottom phase (lipids) were vacuum dried and stored at -80°C. The middle phase was mixed with 200 μl of cold acetone (-20°C), vortexed and centrifuged at 13,000 rpm for 10 minutes. The supernatant was removed, and the remaining pellet was vacuum dried and stored at -80°C.

4.2.6   Protein Digestion and Purification

The protein pellet was resuspended in 10 μl of 10 mM dithiothreitol in 25 mM ammonium bicarbonate and incubated at 37°C for 1 hour to reduce disulfide bonds. The sample was then mixed with 10 μl of alkylation reagent mixture (97.5% acetonitrile, 2% iodoethanol, 0.5% triethylphophine, v/v) and incubated at 37°C for 1 hour. After incubation, the sample was vacuum dried. Then the dry sample was mixed with 80 μl of Lys-C/trypsin mixture (0.05 μg/μl, in 25 mM ammonium bicarbonate) and incubated 37°C in block heater with 1,000 rpm shaking for 12 hours. C18 microspin columns (silica based C18 UltraMicroSpin Column Kit, The Nest Group, Inc.) were conditioned by adding 100 μl 100% acetonitrile and centrifuged for 1 minute at 800 rpm. Then the column was washed twice with 100 μl of double distilled water and centrifuged each time at 1,200 rpm for 1 minute. The digested protein sample was loaded to the conditioned C18 column. The column with sample was centrifuged for

1 minute at 800 rpm, and the liquid was discarded. The column was then washed twice with 100 μl of a solution (0.1% formic acid, 5% acetonitrile, 94.5% double distilled water, v/v), and was centrifuged each time at 1,200 rpm for 1 minute. The column was then placed in a new microcentrifuge tube. The peptides in the column was eluted three time using 50 μl of the elution buffer (0.1% formic acid, 80% acetonitrile, 19.9% double distilled water, v/v) and centrifuge for 1 minute at 1,000 rpm each time. The sample was vacuum dried.

4.2.7   Mass Spectrometry and Mass Spectra Analysis

The concentrations of the peptide samples were determined by using PierceTM BCA Protein Assay Kit (Thermo Scientific). The peptide samples (2 μg/each) were then loaded to Q-Exactive high-field mass spectrometer (Thermo Scientific) and mass spectra data of the samples were obtained. The mass spectra data was first searched against the database consisting of six frame translation of the phage and annotated proteins of *M. smegmatis* by MaxQuant to obtain the list of proteins detected in each sample and label-free quantification (LFQ) intensity.

4.2.8   Developing Linear Regression Model Using SAS

The LFQ intensities of the protein identified and the factor levels (Table 4.2) were further submitted to develop linear regression model which unveiled the numerical correlation between protein expression and each factor using SAS 9.4 (SAS Institute Inc.). The model was displayed in Equation 4.1. The significance of the correlation between each factor and each protein was evaluated by the P value, and only the P value above 0.05 indicates the correlation is significant. The estimates of each factor indicate the correlation level.

Table 4.2.
Factor levels of the experimental design

Factor	Level		
Bacterial growth phases (phase)	Exponential	Stationary	
Phage types (phage)	Negative control	FrenchFry	MrGrodo
Infection time (time, hours)	4	10	

$$E(protein) = \mu + phase_i + phage_j + (phase * phage)_{ij} + time_{kl} + (phase * time)_{ikl}$$
$$+ (phase * time)_{jkl} + (phase * phage * time)_{ijkl} \quad (4.1)$$

4.2.9 Clustering Proteins Identified that Had Significant Correlation with Each Factor

Protein IDs of the proteins that had significant correlation with the factors were submitted to Uniprot for obtaining Gene Ontology (GO) IDs. The GO IDs belong to the same GO categories were counted, and the percentage out of the total number of the proteins were calculated. The GO IDs were subsequently submitted to REVIGO (revigo.irb.hr) to group the GO IDs involved in similar biological process. The allowed similarity on REVIGO was set to medium (0.7).

4.3 Results

4.3.1 Growth Curve of *M. smegmatis*

The growth curve of *M. smegmatis* cell culture indicated that the cell culture reached exponential and stationary growth phases at OD_{600} of about 0.4 and 3.7 (Figure 4.2). Therefore, the exponential cell culture and exponential cell culture

for phage infection would be harvested when the OD_{600} was around 0.4 and 3.7 respectively.

Growth Curve of *M. smegmatis*
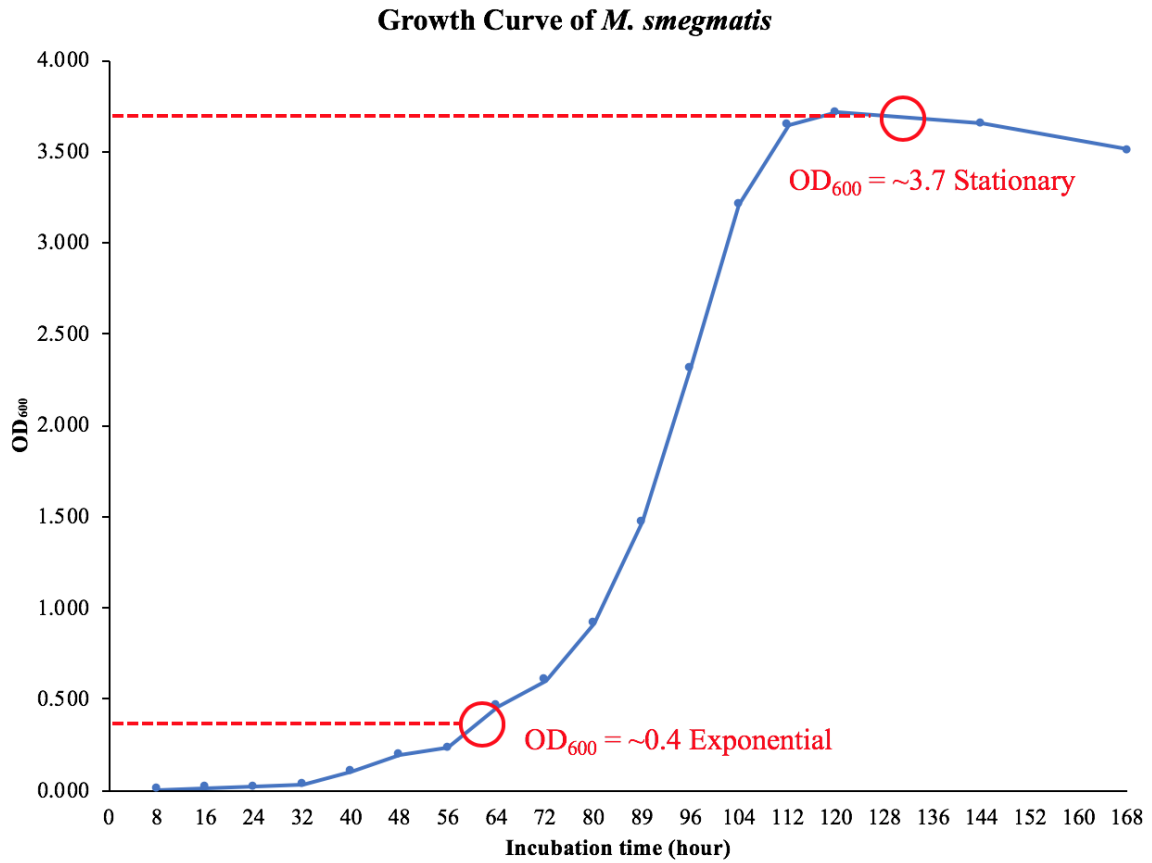
Fig. 4.2. Growth curve of *M. smegmatis* cell culture were determined, and OD_{600} of around 0.4 and 3.7 were chosen as the indicators of exponential and stationary growth phases.

4.3.2   Result of Phage Infection Dynamics

Lytic phages do not possess integrase, thus are not able to initiate lysogenic cycle. The bacterial cells infected by lytic phage were expected to always be lysed and the OD_{600} value of the cell culture must decrease. Temperate phages with integrase have an alternative life cycle in which the phage can integrate genome into bacterial

chromosome and replicate together with the host bacterial cells. Previous researches reported that lysogenic cycle would be preferred when the MOI was over two [78, 79] and the environmental was not favorable for proliferation of host bacterial cells [80]. Therefore, it was expected that the exponential bacterial cell cultures infected by temperate phages had deceasing OD_{600} values, while the stationary cultures had increasing OD_{600} values. Hypothesis of the growth curves of the phage-infected *M. smegmatis* cell cultures was listed in Table 4.3.

Table 4.3.
Hypothesis of growth curves of phage-infected *M. smegmatis* cell cultures

		Infect exponential cell culture		Infect stationary cell culture	
	Type	Cycle	OD_{600}	Cycle	OD_{600}
Cosmolli16	Lytic	Lytic	decrease	Lytic	decrease
FrenchFry	Lytic	Lytic	decrease	Lytic	decrease
Hughesyang	Lytic	Lytic	decrease	Lytic	decrease
JewelBug	Temperate	Lytic	decrease	Lysogenic	increase
MrGordo	Temperate	Lytic	decrease	Lysogenic	increase

The growth curves of the phage-infected exponential *M. smegmatis* cell cultures (Figure 4.3) indicated the OD_{600} change over time. As expected (Table 4.3), Cosmolli16-, Hughesyang-, and MrGordo-infected exponential *M. smegmatis* cells kept growth in the first four hours, and JewelBug-infected cells kept growing in the first three hours. Then the growth of the cells infected by the four phages were depressed. Different from the other four phages, FrenchFry infected the exponentially growing *M. smegmatis* kept growing within the 10 hours of infection. During 4-6 hours of infection, the growth of FrenchFry-infected cell culture slowed down, but after 6 hours, the growth rate increased again.

As shown in Figure 4.4, when the phages infected the stationary *M. smegmatis* cell culture, the OD_{600} value of the cell culture infected by lytic phages Cosmilli16, FrenchFry and Hughesyang did not plunge as expected (Table 4.3). All the phage-infected cell cultures had similar growth curves to the negative control did. The

Growth curve of phage-infected *M. smegmatis* (exponential)
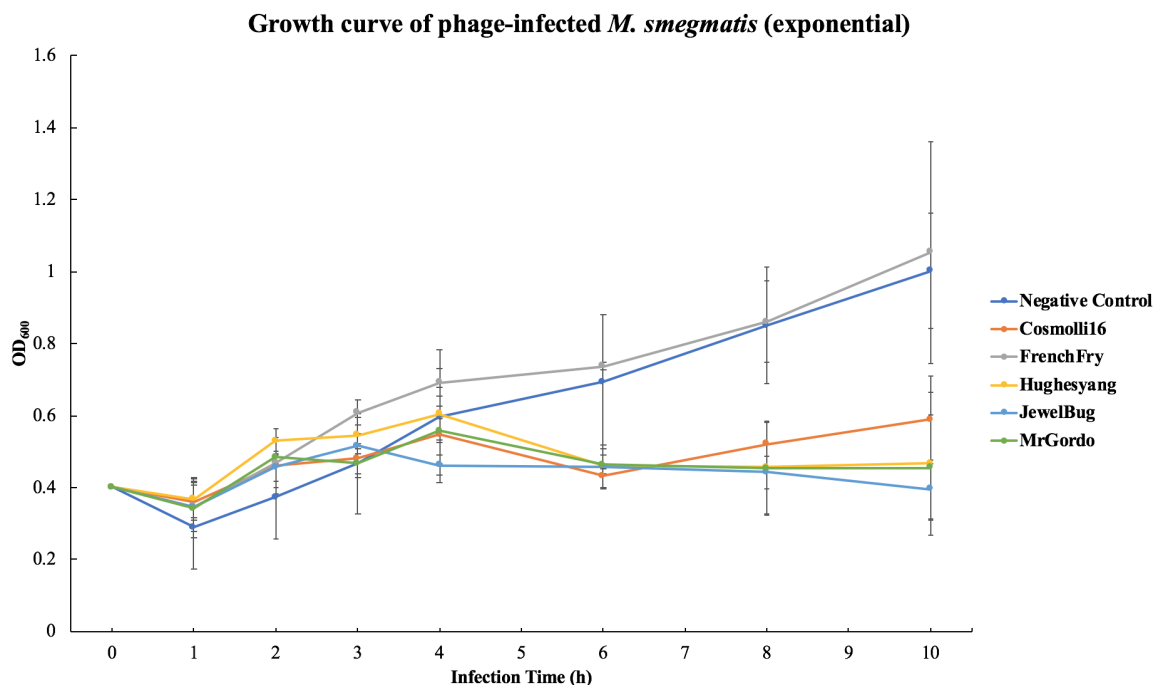
Fig. 4.3. This graph displayed the growth of exponentially growth *M. smegmatis* infected by different phages. Growth rate of M. smegmatis infected by FrenchFry was higher than the cells infected by other phages, and the growth curve was similar to the one of negative control. Compare to the negative control, growth of *M. smegmatis* cell cultures infected by Cosmolli16, Hughesyang, JewelBug and MrGordo were depressed after the first four hours of infection.

OD_{600} values were fluctuated within the range of one and did not have great change at the end of the 10-hour infection compared to the initial values.

Phage titer changes differed during infecting exponential and stationary *M. smegmatis* cell cultures (Figure 4.5). When infecting exponential cell cultures, the phage titers soared and increased more than 104 folds in the first 10 hours. When infecting stationary cell cultures, the phage titer changes varied. Titers of FrenchFry, Hughesyang and MrGordo decreased in the first 10 hours, while titers of Cosmilli16 and JewelBug increased.

Growth curve of phage-infected *M. smegmatis* (stationary)
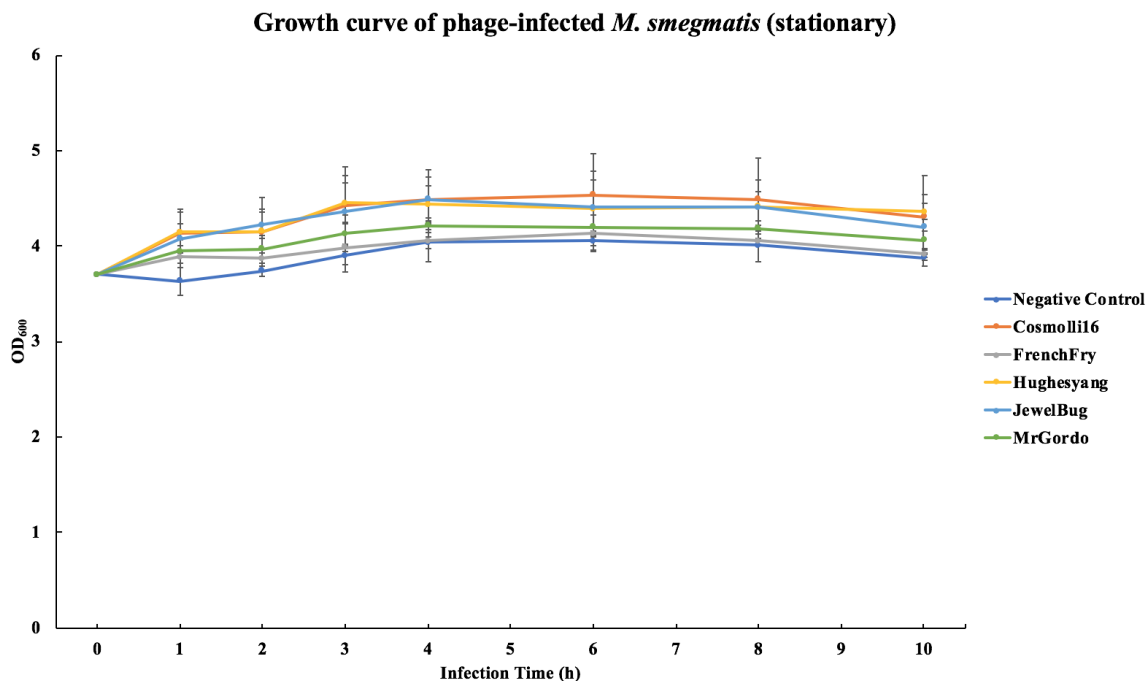
Fig. 4.4. This graph showed OD_{600} change of stationary *M. smegmatis* infected by different phages. Growth curve of *M. smegmatis* infected by different phages were all similar to the growth curve of negative control.

Due to the unexpected growth curve of FrenchFry-infected exponential *M. smegmatis* cell culture, the phage-bacteria mixture were selected for proteins/lipids extraction and subsequent statistical analysis. MrGordo, as a representative temperate phage, was selected as well.

4.3.3 Proteins Significantly Impacted by the Factors

The mass spectra data analyzed by MaxQuant to identify the proteins in each sample. A linear regression model between the LFQ intensity and the factor levels were developed by using SAS program. In the linear regression model of each protein, the factor that had a positive estimate up-regulated the protein, while the factor had a negative estimate down-regulated the protein.
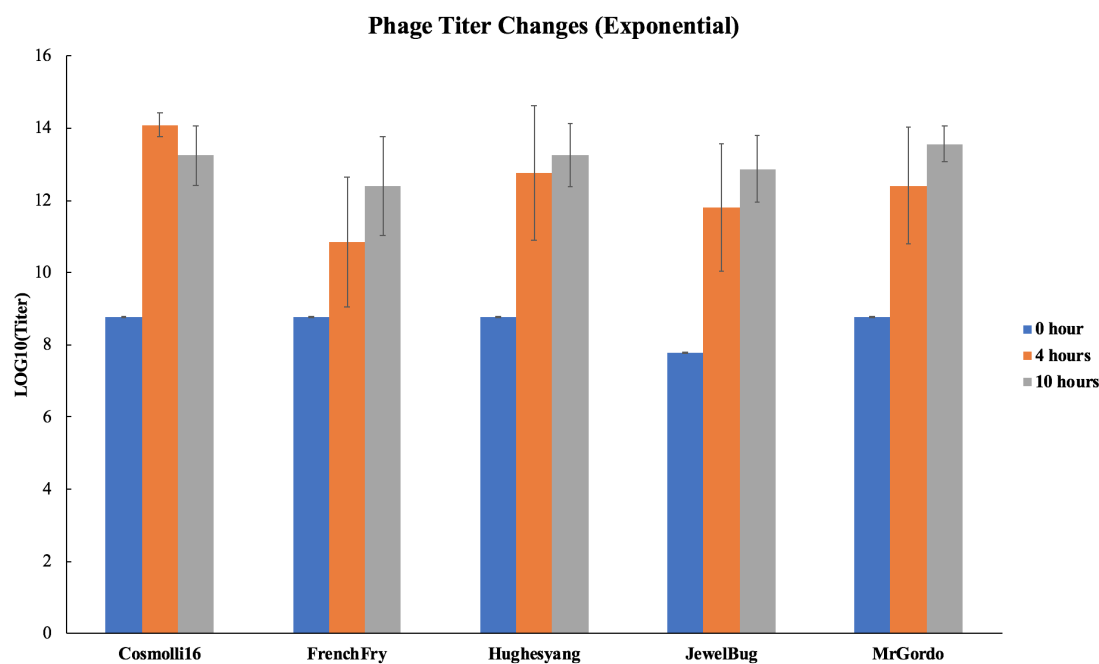
Phage Titer Changes (Exponential)

(a) Phage titer changes when infecting exponentially growing *M. smegmatis* cell cultures

Phage Titer Changes (Stationary)
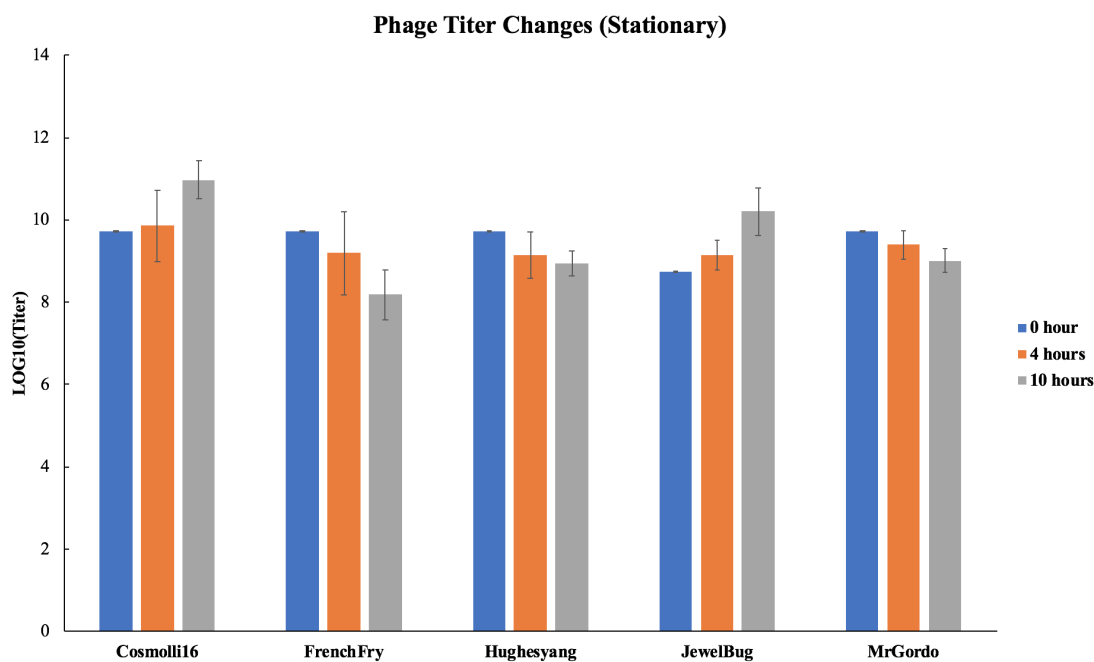
(b) Phage titer changes when infecting stationary growing *M. smegmatis* cell cultures

Fig. 4.5. Phage titer changes when infecting (a) exponentially and (b) stationary growing *M. smegmatis* cell cultures

The Amount of the Proteins Impacted by the Factors

The impact of the different factors on of *M. smegmatis* proteins varied. As shown in Figure 4.6, infection of MrGordo changed expression level of 672 proteins, 34% of which were up-regulated. FrenchFry only impacted 10 proteins and up-regulated two of them. Exponential growth phase and stationary growth phase both stimulated the expression of about 150 proteins. Infection time affected expression of 102 proteins, and 4-hour infection up-regulated three times more proteins than 10-hour infection did.

(a) Proteins impacted by growth phases

(b) Proteins impacted by infection time

(c) Proteins impacted by FrenchFry

(d) Proteins impacted by MrGordo
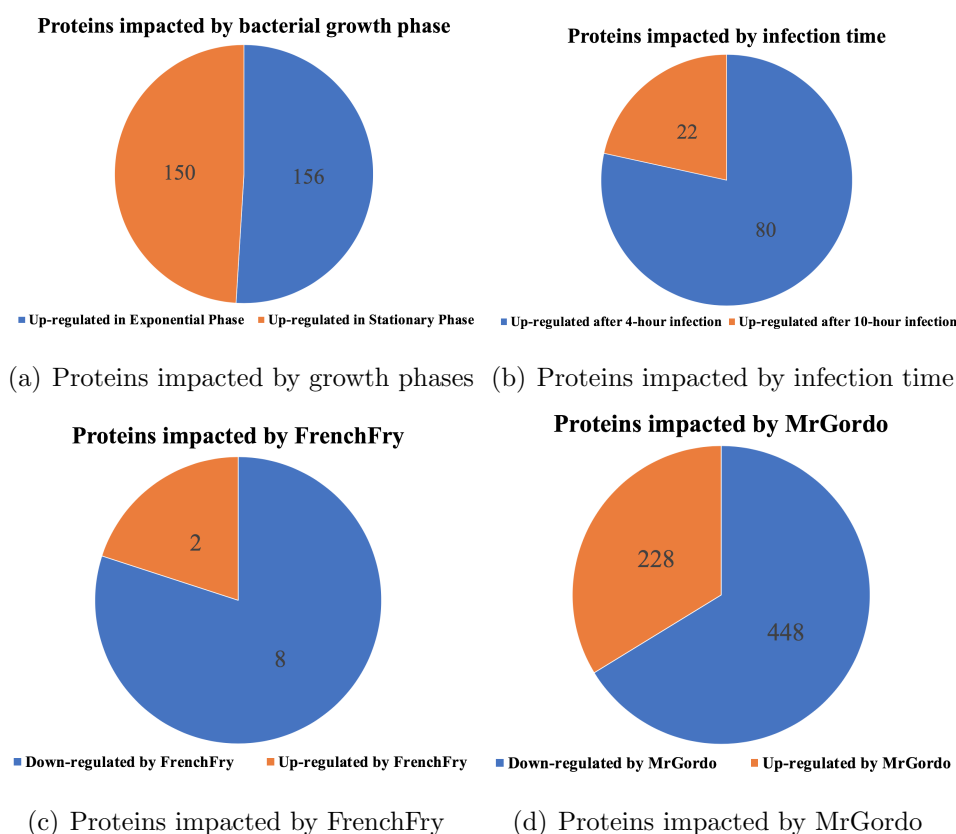
Fig. 4.6. Bacterial growth phases impacted expression of 306 proteins, around 50% of the proteins were up-regulated by either exponential or stationary growth phase. Phage infection time significantly affected 102 proteins, about 78% of the proteins had higher expression level after 4 hours of phage infection. MrGordo, the temperate phage changed expression level of 673 proteins, while FrenchFry, the lytic phage, only changed 10.

Top Ten Proteins Up-/down-regulated by the Factors

Tables A.11-A.18 listed the top ten proteins that were impacted by each factor. Protein IDs and protein names were included in the tables. Protein name also indicated the function of the proteins. The detailed explanation of the protein will be included in next section together with GO groups.

4.3.4 Clustering the Proteins Significantly Impacted by The Factors

GO IDs were used to group the proteins that had similar functions. There are three GO categories: biological process, cellular component and molecular function. Some proteins had GO IDs from multiple GO categories, and the uncharacterized proteins did not have any.

As shown in Figure 4.7, except proteins regulated by FrenchFry (extremely low amount), about 69-87% of the proteins impacted by other factors played roles in molecular function, around 36-59% of them involved in biological processes, and about 23-39% of them located in different cellular components.
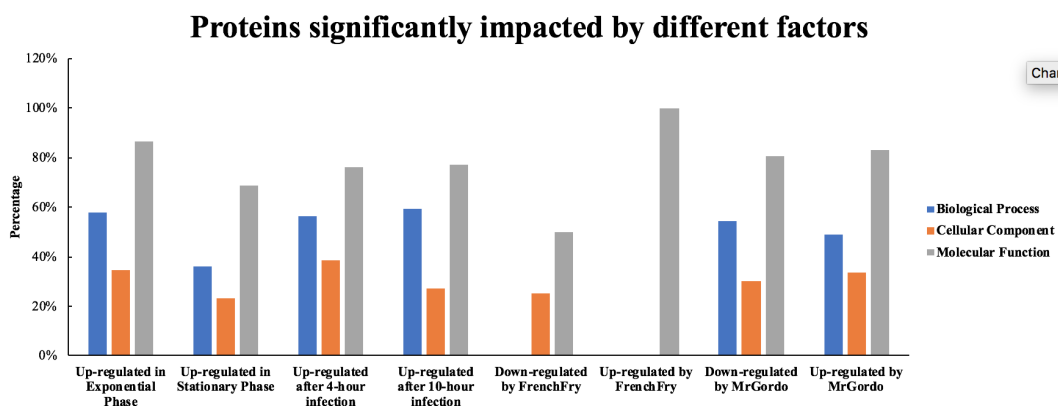
Fig. 4.7. The proteins significantly impacted by the factors were grouped into three categories based on GO IDs. The percentage represents the ration between the number of GO IDs and the number of the proteins significantly impacted by the factors.

As shown in Tables A.19-A.21, in exponentially growing *M. smegmatis* cells, the up-regulated proteins involved in biological processes including cell division, transcription initiation from bacterial-type RNA polymerase promotor and protein pupylation. The up-regulated proteins belonged to integral component of plasma membrane and fatty acid synthase complex. Some of them also occurred in cell division site, extracellular space and periplasmic space. These proteins had molecular functions such as 2-hydroxy-3-oxoadipate synthase activity and cyclohexanone monooxygenase activity.

Protein pupylation is a specific post-translation protein modification found in *M. tubercolusis* [82]. In this process, prokaryotic ubiquitin-like protein (Pup) is conjugated to lysin residues of proteins, which labels the proteins for proteasomal degradation [83]. The up-regulation of the proteins involved in pupylation process indicated that large amount proteins were quickly produced and degraded after accomplishing the biochemical activity. The other up-regulated proteins were involved in cell division, transcription and metabolism. All these biological processes proved that the *M. smegmatis* cells were in the stage with fast cell division and production of new cells.

The proteins also had GO of cellular components belonging to the integral component of plasma membrane and fatty acid synthase complex. The fatty acids biosynthesis is important to the construction of mycobacterial cell wall [84]. In *M. smegmatis* cells, fatty acid synthase complex catalyzes the fatty acid synthesis from acetyl-CoA and malonyl-CoA [85]. Both cellular components categories indicated that these up-regulated proteins involved in new cell formation.

According the Tables A.11 and A.21, the proteins up-regulated by exponential growth phase have the molecular functions of binding to metal ions, uptaking nutrients and catalytic enzyme, which also reflected the impact of exponential growth phase.

As shown in Tables A.22-A.24, in stationary *M. smegmatis* cells, the up-regulated proteins involved in biological processes including one carbon metabolism, response to stress, polyamine transport and tRNA pseudouridine synthesis. The up-regulated proteins belonged to periplasmic space, proteasome complex, integral component of

membrane and extracellular region. These proteins had molecular functions such as dioxygenase activity, fatty acid O-methyltransferase activity and hydrolase acitivty acting on acid carbon-carbon bonds in ketonic substances.

As shown in A.12, luciferase-like protein had a tighter correlation with stationary growth phase. This protein belongs to LLM class F_{420}-dependent oxidoreductase [BIOCYC Database Collection, 2018].

Based on the results in Table A.23, there were two proteins locating in extracellular region, cutinase and fibronectin attachment family protein. Cutin is an insoluble plant glycolipid polymer that consists of hydroxy and epoxy fatty acids [86]. The putative cutinase in *M. smegmatis* acts as a phospholipase A which hydrolyzes phospholipids [87, 88]. The homologous of this protein in *M. tuberculosis*, as one of the lipolytic enzymes, plays an important role in acquisition of host lipids [89] and therefore becomes potential biomarkers for active tuberculosis [90]. Fibronectin is involved in cellular interactions with extracellular matrix and is very important to cell adhesion, migration, growth and differentiation [91]. Fibronectin attachment family protein is expressed in multiple species of mycobacteria participating in attachment and internalization to the host cells [92, 93]. Disruption of fibronectin attachment family protein causes aggregation of *M. smegmatis* cells [94]. *M. smegmatis* cells tend to aggregate due to the waxy hydrophobic cell envelope [95]. Therefore, up-regulation of the two proteins in stationary phase indicated that the cell surface properties of *M. smegmatis* cells changed in stationary phase.

As shown in Tables A.25-A.27, after 4-hour infection, the up-regulated proteins of *M. smegmatis* cells involved in biological processes including cell division, pseudouridine synthesis and protein transport. The up-regulated proteins belonged to periplasmic space, phosphopyruvate hydratase complex and integral component of membrane. These proteins had molecular functions such as biphenyl-2,3-diol1,2-dioxygenase activity, cutinase activity and tRNA binding.

As shown in Table A.13, phosphotyrosine protein phosphatase PtpA mediates *M. tuberculosis* virulence [96], and promotes host cell proliferation and migration [97].

Diacylglycerol O-acyltransferase is involved in production of triacylglycerol which is an energy store for *M. tuberculosis* under stress [98]. Enolase in *M. tuberculosis* is a surface exposed protein that binds to plasminogen host cells and assists infection of *M. tuberculosis* [99, 100].

The up-regulation of these three proteins indicated that phage infection might increase the virulence of the *M. smegmatis*. *M. smegmatis* cells might also start reserve energy when facing stress from phage infection.

As shown in Tables A.28-A.30, after 10-hour infection, the up-regulated proteins of *M. smegmatis* cells involved in biological processes including L-arabinose catabolism to xylulose 5-phosphate, cell wall organization and metabolism. The up-regulated proteins belonged to DNA polymerase III complex and integral component of membrane. These proteins had molecular functions such as penicillin binding glutamyl-tRNA reductase activity, translation release factor activity (codon specific) and ribulokinase activity.

As shown in Table A.14, OsmC family protein belongs to antioxidant category of enzymes and is important to protecting *M. smegmatis* against oxidative stress [101]. Tetratricopetide repeat motifs play an important role in bacterial virulence [102]. folC gene is essential for growth of *M. tuberculosis* [103]. Mutated folC leads to drug resistance in clinical *M. tuberculosis* strains [104, 105].

The up-regulation of these three proteins indicated that after 10 hours of phage infection, virulence and drug resistance of *M. smegmatis* might increase.

As shown in Tables A.31 and A.32, when being infected by FrenchFry, the down-regulated proteins of *M. smegmatis* belonged to integral component of membrane. These proteins played had molecular functions including metal ion binding, metal ion transmembrane transporter activity and ATPase activity.

As shown Tables A.33 and A.34, when being infected by FrenchFry, the up-regulated proteins in *M. smegmatis* had molecular functions of pyridoxal phosphate binding and tryptophan synthase activity.

FrenchFry is a lytic phage, which is supposed to lyse bacterial cells only. However, the growth curve of FrenchFry-infected *M. smegmatis* cells was not depressed as expected, and the population of the cells were very close to the population of cells in negative control over time. Therefore, most of the proteins that involved in cellular components kept the original expression level, and only ten proteins were up-/down-regulated.

The down-regulated proteins located in cell membrane. Since bacterial cells were broken into pieces in the phage lytic cycle, the down-regulation of cell membrane proteins matched the consequences of phage lytic cycle. Coenzyme F_{420}-dependent N5,N10-methenyltetrahydromethanopterin reductase catalysis the reaction in Equation 4.2 [EMBL-EBI, https://www.ebi.ac.uk/QuickGO/term/GO:0018537], which is involved in metabolism of reducing CO_2 to methane [106].

$$5 - methyltetrahydromethanopterin + coenzyme F_{420} + H^+$$
$$= 5, 10 - methylenetetrahydromethanopterin + reduced coenzyme F_{420} \quad (4.2)$$
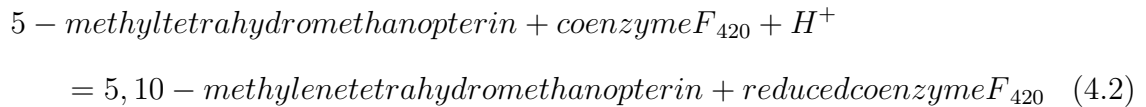
Tryptophan synthase and transcriptional regulator LuxR family were the only two proteins up-regulated during FrenchFry infection (Table A.15). The correlation between FrenchFry infection and tryptophan synthase was very low (estimate was ~ 0.7) while the transcriptional factor (LuxR family) showed tight correlation (estimate was >17). LuxR transcriptional factor plays an important role in quorum sensing (QS) mechanism of M. tuberculosis [107]. QS regulates expression of certain genes with the cell density increase over a threshold [108]. *M. smegmatis* has the LuxR gene, but there is no valid experimental result proving the QS mechanism in *M. smegmatis* yet [109].

As shown in Tables A.35-A.37, when being infected by MrGordo, the down-regulated proteins in *M. smegmatis* involved in biological processes including protein-pyridoxal-5-phosphate linkage via peptidyl-N6-pyridoxal phosphate-L-lysine, carbon fixation and hydrogen peroxide catabolism. The down-regulated proteins cellular

components including glutamyl-tRNA amidotransferase complex, periplasmic space and bacterial nucleoid. These proteins had molecular functions such as formyl-CoA transferase activity, 3-ketosteroid 9-alpha-monooxygenase activity, isoamylase activity and propionate-CoA ligase activity.

Among the proteins down-regulated by MrGordo, dephosphocoenzyme A kinase is the lase enzyme of the Coenzyme A biosynthetic pathway in *M. tuberculosis*, which makes it a potential target for anti-tubercular drug [110]. Transcription elongation factor GreA acting as a chaperon in efficient genome transcription is important for survival of *M. tuberculosis* cells [111]. Glycogen debranching enzyme GlgX of Corynebacterium glutamicum is necessary for degradation of glycogen in response to the hyperosmotic shock [112]. Urease, an important virulence factor in several pathogenic bacteria, plays an important role in nitrogen metabolism of *M. tuberculosis* [113].

As shown in Tables A.38-A.40, when being infected by MrGordo, the up-regulated proteins in *M. smegmatis* cells involved in biological processes including negative regulation of phosphate metabolism, dTDP-rhamnose biosynthesis and cell division. The up-regulated proteins belonged to cellular components including enterobacterin synthetase complex, periplasmic space and cell wall. These proteins had molecular functions such as fatty-acyl-CoA synthase activity, cyclohexanone monooxygenase activity and manganese ion binding.

MCE-family protein (MCE1c) was up-regulated by MrGordo infection. MCE1c similar to MCE1a, is a vital virulence factor of *M. tuberculosis* [114]. Sensor histidine kinase MtrB is a protein of MtrAB two-component signal transduction system that impact cell division and cell wall synthesis in M. tuberculosis [115]. A putative secreted protein (UniProt ID: I7FH47) was also significantly up-regulated, but the function of this protein has not been well studied. Up-regulation of these proteins may indicate that MrGordo infection made *M. smegmatis* cells more virulent.

Proteins of FrenchFry were also detected in the French-infected *M. smegmatis* cell cultures. These proteins were significantly impacted by factors of exponential phase, 4-hour infection and FrenchFry. When infecting exponential *M. smegmatis*

cell culture, gp3 QueC-like queosine biosynthesis, gp6 GTP cyclohydrolase I, gp15 major capsid protein, gp17, gp21 major tail protein, gp24, gp26, gp39 and gp47 lysinA were up-regulated. As shown in Figure 4.5(a), in this process, FrenchFry titer increased which resulted in up-regulation of structural and assembly proteins. After 4-hour infection, gp47 lysinA was up-regulated. It indicated that within the first 4 hours of infection, the FrenchFry was actively lyse *M. smegmatis* cells which led to the increased amount of lysinA.

4.4 Conclusions

4.4.1 Mycobacteriophage Life Cycles Rely on Mycobacterial Growth Phases

Lytic phages were expected to lyse both exponential and stationary *M. smegmatis* cells. However, the growth curve of stationary *M. smegmatis* cell culture infected by the lytic phages proved that the lytic phages did not actively lyse the stationary bacterial cells. Temperate phages are able to enter lysogenic cycle. However, the depressed growth of exponential *M. smegmatis* cell culture infected by the temperate phages proved that the lytic cycle was dominant in this situation. Therefore, the growth phases of *M. smegmatis* altered the phage life cycles of mycobacteriophages.

4.4.2 Both *M. smegmatis* and Mycobacteriophages Are Dynamic Populations During Infection

Exponential *M. smegmatis* cell culture infected by FrenchFry maintained a high growth rate. At the same time, the titer of FrenchFry increased over 104 folds as the other phages did. Thus, both results imply that portion of the *M. smegmatis* cells was actively lysed by FrenchFry and another portion of the cells was still dividing and growing fast, and the cells that kept dividing and growing were the majority. The stationary *M. smegmatis* cell culture infected by Cosmolli16 maintained a high cell population, and the titer of Cosmolli16 increased about 102 folds. It implies

that portion of Cosmolli16 particles entered lytic cycle and lysed the cells, but the Cosmolli16 particles entering lytic cycle were not the majority. Therefore, during mycobacteriophage infection, both *M. smegmatis* cells and mycobacteriophage particles are dynamic populations which consists of different individuals that involve in different activities.

4.4.3 Phage Infection Up-regulated Proteins Related to Mycobacterial Virulence

Factors of 4-hour infection, 10-hour infection and MrGordo infection all up-regulated proteins participating in mycobacterial virulence. As *M. smegmatis* is a non-pathogenic model of *M. tuberculosis*, it is reasonable to assume that *M. tuberculosis* cells infected by mycobacteriophages may become more virulent and tuberculosis cannot be cured.

4.5 Discussions

4.5.1 Stationary Phase May Alter *M. smegmatis* Cell Envelope Composition and Surface Properties

Cutinase and fibronectin attachment family protein were up-regulated in stationary phase. Cutinase hydrolyzes phospholipids and fibronectin attachment family protein reduces cell aggregation. As mycobacterial cell envelope is lipid rich and cells tend to aggregate due to the waxy hydrophobic cell envelope, the up-regulation of the two proteins implies the change of cell envelop composition (especially lipid composition) and subsequent surface properties (less waxy). It was also mentioned in Section 4.4.1 that phage life cycle was altered by the stationary *M. smegmatis* cells. Therefore, it is possible that the special cell envelope composition and surface properties that directly influenced the phage life cycle. To verify this assumption, firstly, the lipid composition of stationary *M. smegmatis* cells need to be investigated, which will be studied and discussed in Chapter 5. Secondly, stationary *M. smegmatis* cell culture

with muted cutinase and fibronectin attachment family protein can be prepared for phage infection. If the cutinase and fibronection attachment family protein deficient cell culture is susceptible for phage infection and OD_{600} value deceases significantly, it means that the two proteins are responsible for the change of cell envelope and the change of cell envelope can alter phage life cycle.

4.5.2 FrenchFry May Trigger A Phage-resistance Mechanism

Growth of exponential *M. smegmatis* cell culture infected by FrenchFry was not depressed as expected. The unusual growth pattern may be caused by up-regulation of LuxR family protein which is a representative protein of QS mechanism. However, the other two lytic phages Cosmolli16 and Hughesyang had different performance. Cosmolli16 and Hughesyang both depressed growth of exponential *M. smegmatis* cell cultures. If there was a QS mechanism directed by LuxR family protein in *M. smegmatis*, the exponential *M. smegmatis* cell cultures infected by Cosmolli116 and Hughesyang should have kept growing as well. Therefore, FrenchFry may be able to initiate a specific phage-resistance mechanism that only works for FrenchFry, and LuxR family protein participates in this mechanism. To verify this assumption, a LuxR deficient *M. smegmatis* strain can be developed for FrenchFry infection. If FrenchFry depress the growth of the LuxR deficient strain, it means the FrenchFry-resistant mechanism does exist.

5. LIPIDOMICS STUDY OF THE IMPACT OF MYCOBACTERIAL PHYSIOLOGY ON MYCOBACTERIOPHAGE LIFE CYCLE

5.1 Introduction

In Chapter 4, both proteins and lipids were extracted from the *M. smegmatis* cell cultures infected by FrenchFry and MrGordo. In this chapter, the lipids of cell will be analyzed by mass spectrometry as well. Linear regression model between amount of each lipid and the experimental factors will be developed. The results will demonstrate (1) the lipids significantly impacted by the experimental factors and (2) the lipids contributing to *M. smegmatis* physiology change.

5.2 Materials and Methods

5.2.1 Mass Spectrometry Analysis

The lipid extracted from FrenchFry- and MrGordo-infected *M. smegmatis* cell culture were dissolved in 50 μl mixture which composed of 50% Eluent A (water, 10 mM ammonium acetate, 0.1% formic acid) and 50% Eluent B (isopropyl alcohol: acetonitrile, 10 mM ammonium acetate, 0.1% formic acid). After centrifuge to remove the remaining particles, the samples (8 μl/sample) were loaded to Waters ACQUITY UPLC® BEH C18 1.7 μm column in Agilent 6545 Q-TOF (Agilent Technologies Inc.) for mass spectrometry analysis. The injection volume was 8 μl/sample. The mass spectra data was further analyzed using MassHunter Profinder B.08.00 (Agilent Technologies Inc.) and Mass Profiler 13.1.1 (Agilent Technologies Inc.). The mass, retention time and intensity of the compounds were obtained.

5.2.2 Developing Linear Regression Model Using SAS

The Log2 normalized intensities of the compounds identified and the factor levels were further submitted to develop linear regression model which unveiled the numerical correlation between the compound intensity and each factor using SAS 9.4 (SAS Institute Inc.). The model was displayed in Equation 5.1. The significance of the correlation between each factor and each compound was evaluated by the P value, and only the P value above 0.05 indicates the correlation is significant. The estimates of each factor indicate the correlation level.

$$E(lipid) = \mu + phase_{i} + phage_{j} + (phase * phage)_{ij} + time_{kl} + (phase * time)_{ikl}$$
$$+ (phase * time)_{jkl} + (phase * phage * time)_{ijkl} \quad (5.1)$$

5.2.3 Identification of The Lipids

The compounds with significant correlation with each factor were then identified by search the mass and retention time against METLIN AM PCDL database in PCDL Manager B.07.00 (Agilent Technologies Inc.). The mass tolerance was 10 ppm, and retention times was optional. The mass of the compounds was further searched in MycoMass Database (Moody Laboratory, Brigham and Womens Hospital) and Mtb Lipid Database (Colorado State University) to identify lipids with the mass tolerance of 0.1. Some compounds had putative attribution from multiple database, then the putative attribution that had the closest mass value was assigned to the compound.

5.3 Results

5.3.1 Amount of the Compounds Identified

The results indicated that 509 compounds were detected in the samples, but only 71 of them showed significant correlation with the factors. As shown in Figure 5.1,

bacterial growth phases had significant impact on 57 compounds, 20 of them were up-regulated in exponential growth phase, and 37 were up-regulated in stationary phase. Phage FrenchFry down-regulated expression of 4 compounds. Infection time impacted 9 compounds, and only one of them was up-regulated after 10 hours of infection.

Lipids impacted by bacterial growth phase

20

37

■ Up-regulated by exponential phase   ■ Up-regulated by stationary phase

(a) Lipids impacted by growth phases

Lipids impacted by infection time

1

8

■ Up-regulated after 4 hour infection   ■ Up-regulated after 10 hour infection

(b) Lipids impacted by Time

Lipids impacted by FrenchFry

0

4

■ Up-regulated   ■ Down-regulated

(c) Lipids impacted by FrenchFry

Fig. 5.1. Total number of compounds that were significantly impacted by each factor.

5.3.2 Putative Attributions of the Detected Compounds

After searching the mass and retention time in three different databases, the putative attributions of part of the compounds were obtained (Tables 5.1-5.4).

Table 5.1.

Putative attributions of the compounds positively correlated with exponential phase

Compound	Formula
Mbt +Fe (R=17:1)	C44H66Fe1N5O10
Latanoprost ethyl amide-d4	C25H35D4NO4
N-arachidonoyl dihydroxypropylamine	C23H39NO3
Lysohosphatidylethanolamine (LPE)	C22H44O7NP
Monoacylglycerol (MAG)	C30H58O4
CAY10573	C33H31NO5
Lysohosphatidylethanolamine (LPE)	C25H52O7NP
UNC0638	C30H47N5O2
Diglyceride (DAG)	C33H62O5
Lysophosphatidylinositol (LPI)	C25H49O12P
Aridanin	C38H61NO8

Triglycerides (TAGs) are main apolar intracellular lipids of *M. tuberculosis* and play a role of energy reserve [51]. TAGs were also found in *M. avium, M. smegmatis* and *M. aurum* [38]. The primary TAG synthase of *M. tuberculosis* (Rv3130c) is a target for drug development [50,98]. In *M. tuberculosis* cells, TAGs are catalyzed by lipolytic enzymes sequentially into diglycerides (DAGs), then to monoacylglycerols (MAGs), and ultimately into free fatty acids. The series of hydrolyzation provides carbon source for energy and synthesis of cell wall components [116].

Table 5.2.

Putative attributions of the compounds positively correlated with stationary phase

Compound	Formula
Lysophosphatidylethanolamines (LPE)	C23H46O7NP
Lysophosphatidylethanolamines (LPE)	C36H72O7NP
(-)-Annonaine	C17H15NO2
Tyr Gly Phe	C20H23N3O5
Ser Ala Cys	C9H17N3O5S
Ritterazine A	C54H76N2O10
Phosphatidic acid (PA)	C45H69O8P
Triglyceride (TAG)	C57H110O6
Triglyceride (TAG)	C59H108O6
Phosphatidylglycerol (PG)	C42H83O10P1
Triglyceride (TAG)	C60H112O6

Table 5.3.

Putative Attributions of the Compounds Positively Correlated with Four-hour Infection

Compound	Formula
Triglyceride (TAG)	C74H138O6
Phosphatidylethanolamine (PE)	C70H138O8NP
Ac2SGL	C61H116O17S
Cardiolipin (CL)	C60H122O17P2
Alpha-Mycolic acid (MA)	C78H152O3
Triglyceride (TAG)	C73H136O6
Phosphatidic acid (PA)	C69H135O8P

Phosphatidylglycerol (PG) and phosphatidylinositol (PI) are both major glycerophospholipids in both *M. tuberculosis* and *M. smegmatis* [40,95] . PI is catabolized via lysophosphatidylinositol (LPI) [117].

Table 5.4.
Putative Attributions of the Compounds Negatively Correlated with
FrenchFry Infection

Compound	Formula
Phosphatidylethanolamine (PE)	C39H76NO8P

Phosphatidylethanolamine (PE) is an important structural polar lipid in cell envelope of mycobacterium species [38, 118]. The functions of PE are still not well known [119]. The enzymes involved in synthesis of PE are the potential target for anti-tuberculosis drugs [120]. It was also reported that PE might enhance activities of multidrug resistant family proteins [121]. Lysophosphatidylethanolamine (LPE), as a component of cell membranes, is converted from PE by phospolipase A [122].

2-palmitoyl or 2-stearoyl-3-hydroxyphthioceranoyl-2'-sulfate-alpha-alpha'-D-trehalose (Ac2SGL) is an intracellular diacylated sulfoglycolipids (SGLs) which are the major virulence lipids of *M. tuberculosis* [123]. Ac2SGL is a competing antagonist that inhibits NF-B activation and cytokine production, which makes the host immune system fail to recognize *M. tuberculosis* [123].

Cardiolipin (CL) is an abundant essential phospholipid in mycobacterial cell membrane [124]. Virulent mycobacterium species have higher content of CL than the saprophytic species [125, 126].

Phosphatidic acids (PA) is an important second messenger that assists assembly and activation of NADPH oxidase, regulates cytoskeleton organization and the vesicular trafficking, and participates in phagocytosis and phagolysosome maturation [127, 128]. PAs are biosynthetic intermediates in *M. tuberculosis* [129], and are precursor of all phospholipids as well [130].

Alpha-Mycolic acid (-MA) is the most abundant class (>70%) of mycolic acids (MAs) that are long-chain fatty acids [131]. MAs are the major components of mycobacterial cell envelope [46] and play an important role in structure and imperme-

ability of the cell envelope [46, 132]. Thus, MA synthesis is one of the targets of antitubercular drugs [133].

Tyr Gly Phe (C20H23N3O5) and Ser Ala Cys (C9H17N3O5S) were metabolites and were detected in *M. tuberculosis* [134–136].

5.3.3 Impact of the Factors on the Lipids Detected

Growth phases had impacts on LPE, LPI, PG, PA, and TAG/DAG/MAG. Four-hour infection increased amount of TAG, PE, Ac2SGL, CL, MA and PA. FrenchFry only showed significant correlation with PE.

In exponential phase, cells actively grow and proliferate, which requires tremendous amount of energy and raw materials to produce progeny cells. The increased intensity of DAG and MAG in exponential phase implied the active hydrolyzation of TAG, the process that provides carbon resource for energy and cell wall formation. In stationary phase, cells have limited nutrients and growth rate slows down. Previous research suggested that the *M. smegmatis* cells can sense the decreasing concentration of surrounding glycerol and uptake remaining glycerol to prepare the adaption to stationary phase [137]. *M. smegmatis* cells in stationary phase is a dynamic population that has a portion of the cells that still actively divide and a portion of the cells that turn dormant [137]. *M. smegmatis* cells in stationary phase also show increased resistance to acid and osmotic stress, which is a prepared for future survival [137]. Therefore, the increase of TAG in stationary phase may indicate that the cells started storing energy to overcome the surrounding stress (especially starvation) and keep alive. The increased intensity of TAG in stationary phase verified the requirement of energy store of cells. As shown in Figure 5.2, TAGs locate in outer membrane, thus the increase of TAGs may also impact phage attachment and subsequent phage life cycle.

Intensity of PA was increased in stationary phase, which might indicate that the cells were producing more phospholipids and subsequent thicker cell envelope.
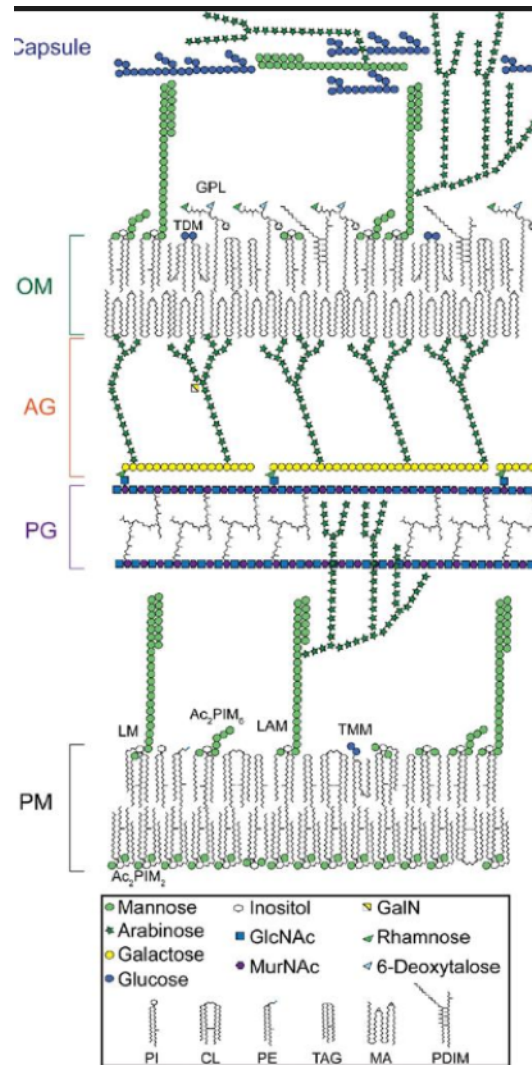
Fig. 5.2. Schematic representation of the mycobacterial cell wall [138].

Four-hour infection allows *M. smegmatis* cells to interact with phages for 4 hours. The increased intensity of Ac2SGL and CL might indicate that the living *M. smegmatis* cells became more virulent. As shown in Figures 5.2 and 5.3, both MAs and acyl glycolipids locate in outer membrane. Thus, it is also possible that the increased component level of Ac2SGL and alpha-MA may impact phage attachment.

Intensity of PE was increased by FrenchFry infection. As shown in Figure 5.3, PEs locate in plasma membrane, and the change of PE content may impact phage genome injection and ultimately change phage life cycle.
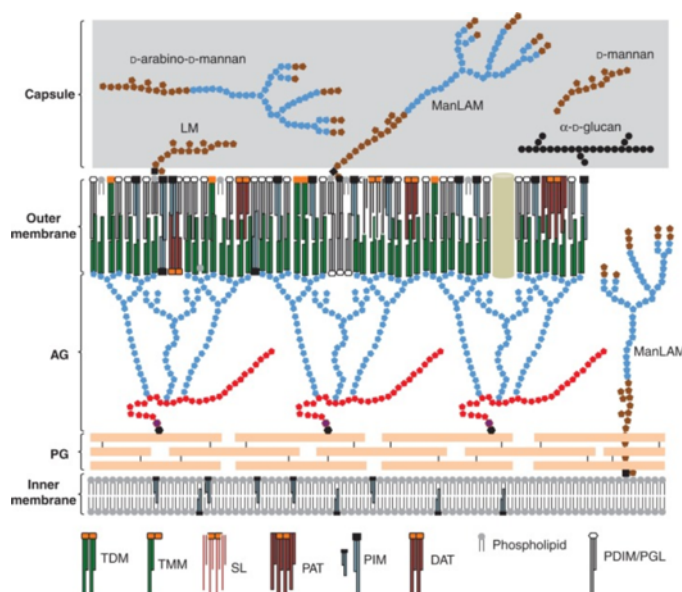
Fig. 5.3. Schematic representation of the *M. tuberculosis* cell envelope [40].

5.4 Conclusions

5.4.1 Bacterial Growth Phase Has Greatest Impact on Lipids

Bacterial growth phase significantly impacted 57 compounds which exceeded other factors. Mycobacterial cell envelope lipid can occupy up to 40% of the dry cell weight [40, 139]. Lots of researches investigated composition of mycobacterial envelope [38, 140], but almost no research explored the cause and impact of lipid composition change. A research in late 1990s reported that *M. tuberculosis* cell wall thickened in stationary phase [141]. Morphology changes of *M. smegmatis* cells in stationary phase were observed using cryo scanning electron microscopy [137]. Therefore, it was expected that the growth phase would have the most significant impact on lipid composition. And the results also supported this hypothesis.

5.4.2   Lipids Composition May Impact Phage Infection Life Cycle

In stationary phase, the *M. smegmatis* cells were not lysed by different phages as expected (results of Chapter 4). And the cell population kept at a high level during the phage infection. In this research stationary phase increased content of structural lipids including LPE, PG and TAG. Since TAGs locate in plasma membrane (Figure 5.2), it is possible that the amount of TAGs can influence phage genome injection and subsequent phage life cycle. FrenchFry increased intensity of PE. And growth of exponential *M. smegmatis* was not depressed by FrenchFry infection (result from Chapter 4), which indicates that lytic cycle was not dominant in this situation. Thus, PE, especially $C_{39}H_{76}NO_8P$ might be the envelope lipid corresponding to life cycle alteration of FrenchFry.

5.4.3   Phage Infection May Increase Virulence of *M. smegmatis*

Four-hour infection increased the infection level of Ac2SGL and CL which have close correlations with mycobacterial virulence.

5.5   Discussions

5.5.1   Extend Lipid Discovery

In this research, only positive ion mode was used. The databases Mycomass and Mtb Lipid employed multiple ionization methods to obtain different types of negative- and positive-ion modes of the lipids. Therefore, in the future, more ionization method will be applied to extend the discovery of lipids that are impacted by each experimental factor.

Lots of detected compounds remained unidentified. Different types of mass spectrometry will be used to verify that these unidentified compounds did present in *M. smegmatis.*

Extend the Studies in Mycobacterial Lipid Composition

As mentioned in Section 5.4.1, the impact of lipid composition change has not been studied a lot. This research unveiled some putative correlations between lipid composition with phage life cycle and with mycobacterial virulence. There are more interesting areas to explore, such as, the lipid composition change during mycobacterial cell proliferation, the lipid composition change in starved mycobacterial cells, and the lipid composition change in the antibiotic-treated mycobacterial cells.

6. CONCLUSIONS AND DISCUSSIONS

6.1 Overview of the Research Project

In this research, a mass spectrometry-based method was developed to study phage proteins in phage-bacteria mixture. Software X! Tandem and database consisting of six frame translation of the phage genome and annotated proteins of *M. smegmatis* was proved to be the best tools for analyzing the mass spectra data. Annotation of phage proteins was verified. Few out-of-frame peptides were detected, which suggested that the start sites of some proteins needed to be extended. Then five phages from diverse clusters were selected to infect *M. smegmatis* cell culture in different exponential and stationary phases. The growth curves of the cell cultures infected by the five phages were determined. Exponential *M. smegmatis* cell culture infected by FrenchFry kept growing, while growth of the exponential cell cultures infected by other four phages were depressed. Stationary cell cultures infected by the five phages maintained a high cell concentration. Total proteins and total lipids were extracted from the cell cultures infected by FrenchFry and MrGordo. Proteomics and lipidomics of the samples were analyzed by mass spectrometry. The correlations between individual proteins/lipids and each experimental factor were investigated by developing linear regression model using SAS. Proteins involved in cell division were up-regulated by exponential phase. Extracellular proteins cutinase and fibronectin attachment family protein were up-regulated by stationary phase. LuxR protein was significantly up-regulated by FrenchFry infection, while expression of over 600 proteins were impacted by MrGordo infection. Proteins associated mycobacterial virulence were up-regulated in both 4-hour and 10-hour infection. Amount of lipids including lysohosphatidylethanolamine (LPE), lysophosphatidylinositol (LPI), phosphatidylglycerol (PG), and phosphatidic acid (PA) were impacted by *M. smegmatis*

growth phases. Four-hour infection increased amount of triglyceride (TAG), phosphatidylethanolamine (PE), Ac2SGL, cardiolipin (CL), mycolic acid (MA) and PA. FrenchFry infection correlated with PE.

6.2 Conclusions

6.2.1 Bacterial Physiology Alters Phage Life Cycles

In this research, the results demonstrated that physiology changes including proteins expression and envelope lipid composition are correlated with growth phases of *M. smegmatis*. The physiology changes alter life cycles of selected phages. When infecting exponential *M. smegmatis* cell culture, the lytic cycle is dominant. When infecting stationary *M. smegmatis* cell culture, the lytic cycle is no longer preferred.

6.2.2 Both *M. smegmatis* and Mycobacteriophages Are Dynamic Populations During Infection

The growth curves of the *M. smegmatis* cell cultures infected by the phages and the titer change of the phages indicated that both *M. smegmatis* cells and mycobacteriophage particles are dynamic populations consisting of different individuals that involve in different activities. In the exponential *M. smegmatis* cell culture, portion of the bacterial cells are actively lysed by FrenchFry and the remaining cells keep growing fast, which ultimately leads to an increasing cell population. In the stationary *M. smegmatis* cell culture, a tiny portion of the bacterial cells are lysed by the phages, the major population turns to be unsusceptible to the infection of the selected five phages. Since only very limited amount of stationary *M. smegmatis* cells can be lysed by the selected phages, only a tiny portion of the phage particles enters lytic cycle. The remaining phage particles may pause infection and stay peacefully together with the *M. smegmatis* cells. Therefore, *M. smegmatis* and mycobacteriophages are dynamic populations during infection.

6.2.3 Phage Infection Improves Virulence of *M. smegmatis*

Proteins and lipids involved in virulence were positively correlated with the 4-hour and 10-hour infections. Since *M. smegmatis* is a non-pathogenic model for studying *M. tuberculosis*, the results may imply that the phage infection can make *M. tuberculosis* more virulent.

6.2.4 Advantage of the Methodology

In this research, the methodology allows to extract and study both total proteins and total lipids together. Although not as many proteins and lipids were detected as expected, both proteomics and lipidomics results led to consistent conclusions. Therefore, the advantages of this methodology include high efficiency and magnifying the of correlation between proteins and lipids.

6.3 Discussions

6.3.1 Phage Therapy Strategies May Need to Be Improved

Current phage therapy uses cocktail of different lytic phages. However, the results of this research showed that the selected lytic phages were not able to eliminate stationary *M. smegmatis* cells. FrenchFry, one of the selected lytic phages even stimulated the growth of exponential *M. smegmatis* cells. Phage infection also up-regulated virulence proteins and increased amount of the lipids associated with virulence. Therefore, in some situations, the phage therapy agents composed of multiple lytic phages may not clear bacterial infection as expected. More specific criteria need to be developed to select phages for phage therapy agents.

6.3.2   Future Studies of Proteins of LuxR, Cutinase and Fibronectin At-tachment Family Protein

Since LuxR was assumed to be vital player in a FrenchFry-resistant mechanism, this assumption needs to be verified and then the mechanism of this resistant mechanism can be studied extensively. Up-regulation of cutinase and fibronectin attachment family protein may change cell surface properties of stationary *M. smegmatis* cells and ultimately make the cells unsusceptible for phage infection. In the future, the cutinase/fibronection attachment family protein deficient *M. smegmatis* strain can be constructed and used for the investigation of both proteins in cell surface properties.

6.3.3   Study Phage-bacteria Interactions in Different Systems

In this research, phage and bacteria were cultivated in growth medium, which is a very simple system. Only bacterial growth phases, phage types and phage infection time were designed in the experiments. Other factors such as temperature, nutrient level and MOI can be studied in the future. In phage therapy, the phages interact with the bacteria cells in human body. The chemicals, human cells and other factors can make phage-bacteria interaction more complicated. In the wild environment, phage-bacteria interaction may be impacted by humidity, temperature and distance between bacteria cells and phage particles. As phage-bacteria interactions and the mechanisms of the interactions are still vague, more complicated systems can be used to study the interactions.

REFERENCES

REFERENCES

[1] M. R. Clokie, A. D. Millard, A. V. Letarov, and S. Heaphy, "Phages in nature," *Bacteriophage*, vol. 1, no. 1, pp. 31–45, 2011.

[2] A. Jurczak-Kurek, T. Gasior, B. Nejman-Faleńczyk, S. Bloch, A. Dydecka, G. Topka, A. Necel, M. Jakubowska-Deredas, M. Narajczyk, M. Richert *et al.*, "Biodiversity of bacteriophages: morphological and biological properties of a large group of phages isolated from urban sewage," *Scientific Reports*, vol. 6, p. 34338, 2016.

[3] E. H. Hankin, "Laction bactericide des eaux de la jumna et du gange sur le vibrion du cholera," *Ann. Inst. Pasteur*, vol. 10, no. 5, p. ll, 1896.

[4] F. W. Twort, "An investigation on the nature of ultra-microscopic viruses." *The Lancet*, vol. 186, no. 4814, pp. 1241–1243, 1915.

[5] F. dHerelle *et al.*, "Sur un microbe invisible antagoniste des bacilles dysentériques," *CR Acad. Sci. Paris*, vol. 165, pp. 373–375, 1917.

[6] H.-W. Ackermann, "5500 phages examined in the electron microscope," *Archives of virology*, vol. 152, no. 2, pp. 227–243, 2007.

[7] T. Marks and R. Sharp, "Bacteriophages and biotechnology: a review," *Journal of Chemical Technology & Biotechnology: International Research in Process, Environmental & Clean Technology*, vol. 75, no. 1, pp. 6–17, 2000.

[8] R. T. Espejo and E. S. Canelo, "Properties of bacteriophage pm2: a lipid-containing bacterial virus," *Virology*, vol. 34, no. 4, pp. 738–747, 1968.

[9] R. SCHÄFER, U. HUBER, and R. M. FRANKLIN, "Chemical and physical properties of mycobacteriophage d29," *European journal of biochemistry*, vol. 73, no. 1, pp. 239–246, 1977.

[10] Ł. Richter, M. Janczuk-Richter, J. Niedziółka-Jönsson, J. Paczesny, and R. Hołyst, "Recent advances in bacteriophage-based methods for bacteria detection," *Drug discovery today*, 2017.

[11] W. Cenens, A. Makumi, M. T. Mebrhatu, R. Lavigne, and A. Aertsen, "Phage–host interactions during pseudolysogeny: Lessons from the pid/dgo interaction," *Bacteriophage*, vol. 3, no. 1, p. e1003269, 2013.

[12] J. H. Paul and S. C. Jiang, "Lysogeny and transduction," *Methods in microbiology*, pp. 105–128, 2001.

[13] A. Towse, C. K. Hoyle, J. Goodall, M. Hirsch, J. Mestre-Ferrandiz, and J. H. Rex, "Time for a change in how new antibiotics are reimbursed: Development of an insurance framework for funding new antibiotics based on a policy of risk mitigation," *Health Policy*, vol. 121, no. 10, pp. 1025–1030, 2017.

[14] C. Loc-Carrillo and S. T. Abedon, "Pros and cons of phage therapy," *Bacteriophage*, vol. 1, no. 2, pp. 111–114, 2011.

[15] G. F. Hatfull, "Mycobacteriophages: windows into tuberculosis," *PLoS pathogens*, vol. 10, no. 3, p. e1003953, 2014.

[16] M. W. Taylor, "Phage therapy and the future," in *Viruses and Man: A History of Interactions*. Springer, 2014, pp. 309–319.

[17] T. B. Rice, "The use of bacteriophage filtrates in the treatment of suppurative conditions," *The American Journal of the Medical Sciences*, vol. 179, no. 3, pp. 345–360, 1930.

[18] T. Hausler, "Viruses versus, superbugs," 2006.

[19] A. Sulakvelidze, Z. Alavidze, and J. G. Morris, "Bacteriophage therapy," *Antimicrobial agents and chemotherapy*, vol. 45, no. 3, pp. 649–659, 2001.

[20] B. Weber-Dabrowska, M. Dabrowski, and S. Slopek, "Studies on bacteriophage penetration in patients subjected to phage therapy." *Archivum immunologiae et therapiae experimentalis*, vol. 35, no. 5, pp. 563–568, 1987.

[21] Y. Yang, F. Xu, H. Xu, Z. P. Aguilar, R. Niu, Y. Yuan, J. Sun, X. You, W. Lai, Y. Xiong *et al.*, "Magnetic nano-beads based separation combined with propidium monoazide treatment and multiplex pcr assay for simultaneous detection of viable salmonella typhimurium, escherichia coli o157: H7 and listeria monocytogenes in food products," *Food microbiology*, vol. 34, no. 2, pp. 418–424, 2013.

[22] J. Kuhn, M. Suissa, J. Wyse, I. Cohen, I. Weiser, S. Reznick, S. Lubinsky-Mink, G. Stewart, and S. Ulitzur, "Detection of bacteria using foreign dna: the development of a bacteriophage reagent for salmonella," *International journal of food microbiology*, vol. 74, no. 3, pp. 229–238, 2002.

[23] S. Ulitzur, J. Kuhn *et al.*, "Introduction of lux genes into bacteria, a new approach for specific determination of bacteria and their antibiotic susceptibility," *Bioluminescence and chemiluminescence new perspectives. Wiley, New York*, pp. 463–472, 1987.

[24] S. Ripp, P. Jegier, M. Birmele, C. Johnson, K. Daumer, J. Garland, and G. Sayler, "Linking bacteriophage infection to quorum sensing signalling and bioluminescent bioreporter monitoring for direct detection of bacterial agents," *Journal of applied microbiology*, vol. 100, no. 3, pp. 488–499, 2006.

[25] G. F. Hatfull, "The secret lives of mycobacteriophages," in *Advances in virus research*. Elsevier, 2012, vol. 82, pp. 179–288.

[26] W. H. Pope, C. A. Bowman, D. A. Russell, D. Jacobs-Sera, D. J. Asai, S. G. Cresawn, W. R. Jacobs Jr, R. W. Hendrix, J. G. Lawrence, G. F. Hatfull *et al.*, "Whole genome comparison of a large collection of mycobacteriophages reveals a continuum of phage genetic diversity," *Elife*, vol. 4, p. e06416, 2015.

[27] W. D. Jones, H. L. David, and R. E. Beam, "The occurrence of lipids in my-cobacteriophage d29 propagated in mycobacterium smegmatis atcc 607," *American Review of Respiratory Disease*, vol. 102, no. 5, pp. 814–817, 1970.

[28] B. Bowman, H. Newman, J. Moritz, and R. Koehler, "Properties of mycobacte-riophage ds6a: Ii. lipid composition," *American Review of Respiratory Disease*, vol. 107, no. 1, pp. 42–49, 1973.

[29] D. Fay and B. Bowman, "Bacteriol proc." 1971.

[30] M. Ventura, C. Canchaya, A. Tauch, G. Chandra, G. F. Fitzgerald, K. F. Chater, and D. van Sinderen, "Genomics of actinobacteria: tracing the evo-lutionary history of an ancient phylum," *Microbiology and molecular biology reviews*, vol. 71, no. 3, pp. 495–548, 2007.

[31] G. M. Cook, M. Berney, S. Gebhard, M. Heinemann, R. A. Cox, O. Danilchanka, and M. Niederweis, "Physiology of mycobacteria," *Advances in microbial phys-iology*, vol. 55, pp. 81–319, 2009.

[32] P. J. Brennan, "Structure, function, and biogenesis of the cell wall of mycobac-terium tuberculosis," *Tuberculosis*, vol. 83, no. 1-3, pp. 91–97, 2003.

[33] E. C. Hett and E. J. Rubin, "Bacterial growth and cell division: a mycobacterial perspective," *Microbiology and Molecular Biology Reviews*, vol. 72, no. 1, pp. 126–156, 2008.

[34] P. J. Brennan and H. Nikaido, "The envelope of mycobacteria," *Annual review of biochemistry*, vol. 64, no. 1, pp. 29–63, 1995.

[35] C. L. Cosma, D. R. Sherman, and L. Ramakrishnan, "The secret lives of the pathogenic mycobacteria," *Annual Reviews in Microbiology*, vol. 57, no. 1, pp. 641–676, 2003.

[36] A. G. Klann, A. E. Belanger, A. Abanes-De Mello, J. Y. Lee, and G. F. Hatfull, "Characterization of the dnag locus inmycobacterium smegmatis reveals linkage of dna replication and cell division," *Journal of bacteriology*, vol. 180, no. 1, pp. 65–72, 1998.

[37] R. O'Toole, "Experimental models used to study human tuberculosis," in *Ad-vances in applied microbiology*. Elsevier, 2010, vol. 71, pp. 75–89.

[38] A. Ortalo-Magne, A. Lemassu, M.-A. Laneelle, F. Bardou, G. Silve, P. Gounon, G. Marchal, and M. Daffé, "Identification of the surface-exposed lipids on the cell envelopes of mycobacterium tuberculosis and other mycobacterial species." *Journal of bacteriology*, vol. 178, no. 2, pp. 456–461, 1996.

[39] Z. He and J. De Buck, "Cell wall proteome analysis of mycobacterium smeg-matis strain mc2 155," *BMC microbiology*, vol. 10, no. 1, p. 121, 2010.

[40] M. Jackson, "The mycobacterial cell envelopelipids," *Cold Spring Harbor per-spectives in medicine*, p. a021105, 2014.

[41] W. R. Butler and L. S. Guthertz, "Mycolic acid analysis by high-performance liquid chromatography for identification of mycobacterium species," *Clinical microbiology reviews*, vol. 14, no. 4, pp. 704–726, 2001.

[42] E. Layre, L. Sweet, S. Hong, C. A. Madigan, D. Desjardins, D. C. Young, T.-Y. Cheng, J. W. Annand, K. Kim, I. C. Shamputa *et al.*, "A comparative lipidomics platform for chemotaxonomic analysis of mycobacterium tuberculosis," *Chemistry & biology*, vol. 18, no. 12, pp. 1537–1549, 2011.

[43] E. D. Chow and J. S. Cox, "Tb lipidomicsthe final frontier," *Chemistry & biology*, vol. 18, no. 12, pp. 1517–1518, 2011.

[44] P. J. Crick and X. L. Guan, "Lipid metabolism in mycobacteriainsights using mass spectrometry-based lipidomics," *Biochimica et Biophysica Acta (BBA)-Molecular and Cell Biology of Lipids*, vol. 1861, no. 1, pp. 60–67, 2016.

[45] H. Marrakchi, M.-A. Lanéelle, and M. Daffé, "Mycolic acids: structures, biosynthesis, and beyond," *Chemistry & biology*, vol. 21, no. 1, pp. 67–85, 2014.

[46] M. Daffé and P. Draper, "The envelope layers of mycobacteria with reference to their pathogenicity," in *Advances in microbial physiology*. Elsevier, 1997, vol. 39, pp. 131–203.

[47] X. Han, *Lipidomics: Comprehensive mass spectrometry of lipids*. John Wiley & Sons, 2016.

[48] D. Sambandan, D. N. Dao, B. C. Weinrick, C. Vilchèze, S. S. Gurcha, A. Ojha, L. Kremer, G. S. Besra, G. F. Hatfull, and W. R. Jacobs, "Keto-mycolic acid-dependent pellicle formation confers tolerance to drug-sensitive mycobacterium tuberculosis," *MBio*, vol. 4, no. 3, pp. e00 222–13, 2013.

[49] A. K. Ojha, X. Trivelli, Y. Guerardel, L. Kremer, and G. F. Hatfull, "Enzymatic hydrolysis of trehalose dimycolate releases free mycolic acids during mycobacterial growth in biofilms," *Journal of Biological Chemistry*, vol. 285, no. 23, pp. 17 380–17 389, 2010.

[50] J. Daniel, C. Deb, V. S. Dubey, T. D. Sirakova, B. Abomoelak, H. R. Morbidoni, and P. E. Kolattukudy, "Induction of a novel class of diacylglycerol acyltransferases and triacylglycerol accumulation in mycobacterium tuberculosis as it goes into a dormancy-like state in culture," *Journal of bacteriology*, vol. 186, no. 15, pp. 5017–5030, 2004.

[51] P. Brennan, "Mycobacterium and other actinomycetes," *Microbial lipids*, vol. 1, pp. 203–298, 1988.

[52] A. Eldar and M. B. Elowitz, "Functional roles for noise in genetic circuits," *Nature*, vol. 467, no. 7312, p. 167, 2010.

[53] G. Balázsi, A. van Oudenaarden, and J. J. Collins, "Cellular decision making and biological noise: from microbes to mammals," *Cell*, vol. 144, no. 6, pp. 910–925, 2011.

[54] N. Dhar and J. D. McKinney, "Microbial phenotypic heterogeneity and antibiotic tolerance," *Current opinion in microbiology*, vol. 10, no. 1, pp. 30–38, 2007.

[55] K. Lewis, "Persister cells," *Annual review of microbiology*, vol. 64, pp. 357–372, 2010.

[56] N. Balaban, "Persistence: mechanisms for triggering and enhancing phenotypic variability," *Current opinion in genetics & development*, vol. 21, no. 6, pp. 768–775, 2011.

[57] G. L. Hobby, K. Meyer, and E. Chaffee, "Observations on the mechanism of action of penicillin." *Proceedings of the Society for Experimental Biology and Medicine*, vol. 50, no. 2, pp. 281–285, 1942.

[58] G. L. Hobby and M. H. Dawson, "Effect of rate of growth of bacteria on action of penicillin." *Proceedings of the Society for Experimental Biology and Medicine*, vol. 56, no. 2, pp. 181–184, 1944.

[59] E. L. Kussell, R. Kishony, N. Q. Balaban, and S. Leibler, "Bacterial persistence: a model of survival in changing environments," *Genetics*, 2005.

[60] Y. Wakamoto, N. Dhar, R. Chait, K. Schneider, F. Signorino-Gelo, S. Leibler, and J. D. McKinney, "Dynamic persistence of antibiotic-stressed mycobacteria," *Science*, vol. 339, no. 6115, pp. 91–95, 2013.

[61] N. H. Keep, J. M. Ward, M. Cohen-Gonsaud, and B. Henderson, "Wake up! peptidoglycan lysis and bacterial non-growth states," *Trends in microbiology*, vol. 14, no. 6, pp. 271–276, 2006.

[62] P. J. Piggot and D. W. Hilbert, "Sporulation of bacillus subtilis," *Current opinion in microbiology*, vol. 7, no. 6, pp. 579–586, 2004.

[63] M. Barer, "Physiological and molecular aspects of growth, non-growth, culturability and viability in bacteria," in *Dormancy and low-growth states in microbial disease*. Cambridge University Press, 2003, pp. 1–35.

[64] H.-S. Xu, N. Roberts, F. Singleton, R. Attwell, D. Grimes, and R. Colwell, "Survival and viability of nonculturableescherichia coli andvibrio cholerae in the estuarine and marine environment," *Microbial ecology*, vol. 8, no. 4, pp. 313–323, 1982.

[65] Y. Hu, A. R. Coates, and D. A. Mitchison, "Sterilizing activities of fluoroquinolones against rifampin-tolerant populations of mycobacterium tuberculosis," *Antimicrobial agents and chemotherapy*, vol. 47, no. 2, pp. 653–657, 2003.

[66] P. Rice, I. Longden, and A. Bleasby, "Emboss: the european molecular biology open software suite," *Trends in genetics*, vol. 16, no. 6, pp. 276–277, 2000.

[67] M. C. Chambers, B. Maclean, R. Burke, D. Amodei, D. L. Ruderman, S. Neumann, L. Gatto, B. Fischer, B. Pratt, J. Egertson *et al.*, "A cross-platform toolkit for mass spectrometry and proteomics," *Nature biotechnology*, vol. 30, no. 10, p. 918, 2012.

[68] W. H. Pope, D. Jacobs-Sera, D. A. Russell, D. H. Rubin, A. Kajee, Z. N. Msibi, M. H. Larsen, W. R. Jacobs, J. G. Lawrence, R. W. Hendrix *et al.*, "Genomics and proteomics of mycobacteriophage patience, an accidental tourist in the mycobacterium neighborhood," *MBio*, vol. 5, no. 6, pp. e02 145–14, 2014.

[69] J. Mehla, R. M. Dedrick, J. H. Caufield, R. Siefring, M. Mair, A. Johnson, G. F. Hatfull, and P. Uetz, "The protein interactome of mycobacteriophage giles predicts functions for unknown proteins," *Journal of bacteriology*, pp. JB–00 164, 2015.

[70] S. G. Cresawn, M. Bogel, N. Day, D. Jacobs-Sera, R. W. Hendrix, and G. F. Hatfull, "Phamerator: a bioinformatic tool for comparative bacteriophage genomics," *BMC bioinformatics*, vol. 12, no. 1, p. 395, 2011.

[71] M. J. Catalão, C. Milho, F. Gil, J. Moniz-Pereira, and M. Pimentel, "A second endolysin gene is fully embedded in-frame with the lysa gene of mycobacteriophage ms6," *PLoS One*, vol. 6, no. 6, p. e20515, 2011.

[72] M. Henry, M. Begley, H. Neve, F. Maher, R. P. Ross, O. McAuliffe, A. Coffey, and J. M. O'Mahony, "Cloning and expression of a mureinolytic enzyme from the mycobacteriophage tm4," *FEMS microbiology letters*, vol. 311, no. 2, pp. 126–132, 2010.

[73] J. C. Van Kessel and G. F. Hatfull, "Recombineering in mycobacterium tuberculosis," *Nature methods*, vol. 4, no. 2, p. 147, 2007.

[74] D. Nelson, R. Schuch, P. Chahales, S. Zhu, and V. A. Fischetti, "Plyc: a multimeric bacteriophage lysin," *Proceedings of the National Academy of Sciences*, vol. 103, no. 28, pp. 10 765–10 770, 2006.

[75] S. Kanamaru, Y. Ishiwata, T. Suzuki, M. G. Rossmann, and F. Arisaka, "Control of bacteriophage t4 tail lysozyme activity during the infection process," *Journal of molecular biology*, vol. 346, no. 4, pp. 1013–1020, 2005.

[76] M. Xu, A. Arulandu, D. K. Struck, S. Swanson, J. C. Sacchettini, and R. Young, "Disulfide isomerization after membrane release of its sar domain activates p1 lysozyme," *Science*, vol. 307, no. 5706, pp. 113–117, 2005.

[77] A. A. Pohane, H. Joshi, and V. Jain, "Molecular dissection of phage endolysin: an interdomain interaction confers host specificity in lysin a of mycobacterium phage d29," *Journal of Biological Chemistry*, pp. jbc–M113, 2014.

[78] A. B. Oppenheim, O. Kobiler, J. Stavans, D. L. Court, and S. Adhya, "Switches in bacteriophage lambda development," *Annu. Rev. Genet.*, vol. 39, pp. 409–429, 2005.

[79] P. Kourilsky, "Lysogenization by bacteriophage lambda," *Molecular and General Genetics MGG*, vol. 122, no. 2, pp. 183–195, 1973.

[80] P. Marsh and E. Wellington, "Phage-host interactions in soil," *FEMS Microbiology Ecology*, vol. 15, no. 1-2, pp. 99–107, 1994.

[81] F. St-Pierre and D. Endy, "Determination of cell fate selection during phage lambda infection," *Proceedings of the National Academy of Sciences*, vol. 105, no. 52, pp. 20 705–20 710, 2008.

[82] M. J. Pearce, J. Mintseris, J. Ferreyra, S. P. Gygi, and K. H. Darwin, "Ubiquitin-like protein involved in the proteasome pathway of mycobacterium tuberculosis," *Science*, vol. 322, no. 5904, pp. 1104–1107, 2008.

[83] J. Barandun, C. L. Delley, and E. Weber-Ban, "The pupylation pathway and its role in mycobacteria," *BMC biology*, vol. 10, no. 1, p. 95, 2012.

[84] R. J. Kinsella, D. A. Fitzpatrick, C. J. Creevey, and J. O. McInerney, "Fatty acid biosynthesis in mycobacterium tuberculosis: lateral gene transfer, adaptive evolution, and gene duplication," *Proceedings of the National Academy of Sciences*, vol. 100, no. 18, pp. 10 320–10 325, 2003.

[85] D. Peterson and K. Bloch, "Mycobacterium smegmatis fatty acid synthetase. long chain transacylase chain length specificity." *Journal of Biological Chemistry*, vol. 252, no. 16, pp. 5735–5739, 1977.

[86] W. Fett, H. Gerard, R. Moreau, S. Osman, and L. Jones, "Screening of non-filamentous bacteria for production of cutin-degrading enzymes," *Applied and environmental microbiology*, vol. 58, no. 7, pp. 2123–2130, 1992.

[87] N. P. West, F. M. Chow, E. J. Randall, J. Wu, J. Chen, J. M. Ribeiro, and W. J. Britton, "Cutinase-like proteins of mycobacterium tuberculosis: characterization of their variable enzymatic functions and active site identification," *The FASEB Journal*, vol. 23, no. 6, pp. 1694–1704, 2009.

[88] S. K. Parker, K. M. Curtin, and M. L. Vasil, "Purification and characterization of mycobacterial phospholipase a: an activity associated with mycobacterial cutinase," *Journal of bacteriology*, vol. 189, no. 11, pp. 4153–4160, 2007.

[89] K. Côtes, J. B. Ngoma, R. Dhouib, I. Douchet, D. Maurin, F. Carrière, and S. Canaan, "Lipolytic enzymes in mycobacterium tuberculosis," *Applied microbiology and biotechnology*, vol. 78, no. 5, p. 741, 2008.

[90] B. Brust, M. Lecoufle, E. Tuaillon, L. Dedieu, S. Canaan, V. Valverde, and L. Kremer, "Mycobacterium tuberculosis lipolytic enzymes as potential biomarkers for the diagnosis of active tuberculosis," *PloS one*, vol. 6, no. 9, p. e25078, 2011.

[91] R. Pankov and K. M. Yamada, "Fibronectin at a glance," *Journal of cell science*, vol. 115, no. 20, pp. 3861–3863, 2002.

[92] T. Secott, T. Lin, and C. Wu, "Fibronectin attachment protein homologue mediates fibronectin binding by mycobacterium avium subsp. paratuberculosis," *Infection and immunity*, vol. 69, no. 4, pp. 2075–2082, 2001.

[93] ——, "Fibronectin attachment protein is necessary for efficient attachment and invasion of epithelial cells by mycobacterium avium subsp. paratuberculosis," *Infection and immunity*, vol. 70, no. 5, pp. 2670–2675, 2002.

[94] Y. Miyamoto, T. Mukai, F. Takeshita, N. Nakata, Y. Maeda, M. Kai, and M. Makino, "Aggregation of mycobacteria caused by disruption of fibronectin-attachment protein-encoding gene," *FEMS microbiology letters*, vol. 236, no. 2, pp. 227–234, 2004.

[95] C. Villeneuve, M. Gilleron, I. Maridonneau-Parini, M. Daffé, C. Astarie-Dequeker, and G. Etienne, "Mycobacteria use their surface-exposed glycolipids to infect human macrophages through a receptor-dependent process," *Journal of lipid research*, vol. 46, no. 3, pp. 475–483, 2005.

[96] H. Bach, K. G. Papavinasasundaram, D. Wong, Z. Hmama, and Y. Av-Gay, "Mycobacterium tuberculosis virulence is mediated by ptpa dephosphorylation of human vacuolar protein sorting 33b," *Cell host & microbe*, vol. 3, no. 5, pp. 316–322, 2008.

[97] J. Wang, P. Ge, L. Qiang, F. Tian, D. Zhao, Q. Chai, M. Zhu, R. Zhou, G. Meng, Y. Iwakura *et al.*, "The mycobacterial phosphatase ptpa regulates the expression of host genes and promotes cell proliferation," *Nature communications*, vol. 8, no. 1, p. 244, 2017.

[98] T. D. Sirakova, V. S. Dubey, C. Deb, J. Daniel, T. A. Korotkova, B. Abomoelak, and P. E. Kolattukudy, "Identification of a diacylglycerol acyltransferase gene involved in accumulation of triacylglycerol in mycobacterium tuberculosis under stress," *Microbiology*, vol. 152, no. 9, pp. 2717–2725, 2006.

[99] A. Rahi, S. K. Matta, A. Dhiman, J. Garhyan, M. Gopalani, S. Chandra, and R. Bhatnagar, "Enolase of mycobacterium tuberculosis is a surface exposed plasminogen binding protein," *Biochimica et Biophysica Acta (BBA)-General Subjects*, vol. 1861, no. 1, pp. 3355–3364, 2017.

[100] A. Rahi, A. Dhiman, D. Singh, A. M. Lynn, M. Rehan, and R. Bhatnagar, "Exploring the interaction between mycobacterium tuberculosis enolase and human plasminogen using computational methods and experimental techniques," *Journal of cellular biochemistry*, vol. 119, no. 2, pp. 2408–2417, 2018.

[101] S. Saikolappan, K. Das, S. J. Sasindran, C. Jagannath, and S. Dhandayuthapani, "Osmc proteins of mycobacterium tuberculosis and mycobacterium smegmatis protect against organic hydroperoxide stress," *Tuberculosis*, vol. 91, pp. S119–S127, 2011.

[102] L. Cerveny, A. Straskova, V. Dankova, A. Hartlova, M. Ceckova, F. Staud, and J. Stulik, "Tetratricopeptide repeat motifs in the world of bacterial pathogens: role in virulence mechanisms," *Infection and immunity*, vol. 81, no. 3, pp. 629–635, 2013.

[103] H. Zhang, D. Li, L. Zhao, J. Fleming, N. Lin, T. Wang, Z. Liu, C. Li, N. Galwey, J. Deng *et al.*, "Genome sequencing of 161 mycobacterium tuberculosis isolates from china identifies genes and intergenic regions associated with drug resistance," *Nature genetics*, vol. 45, no. 10, p. 1255, 2013.

[104] F. Zhao, X.-D. Wang, L. N. Erber, M. Luo, A.-z. Guo, S.-s. Yang, J. Gu, B. J. Turman, Y.-r. Gao, D.-f. Li *et al.*, "Binding pocket alterations in dihydrofolate synthase confer resistance to para-aminosalicylic acid in clinical isolates of mycobacterium tuberculosis," *Antimicrobial agents and chemotherapy*, vol. 58, no. 3, pp. 1479–1487, 2014.

[105] N. Dookie, S. Rambaran, N. Padayatchi, S. Mahomed, and K. Naidoo, "Evolution of drug resistance in mycobacterium tuberculosis: a review on the molecular determinants of resistance and implications for personalized care," *Journal of Antimicrobial Chemotherapy*, vol. 73, no. 5, pp. 1138–1151, 2018.

[106] S. W. Aufhammer, E. Warkentin, U. Ermler, C. H. Hagemeier, R. K. Thauer, and S. Shima, "Crystal structure of methylenetetrahydromethanopterin reductase (mer) in complex with coenzyme f420: Architecture of the f420/fmn binding site of enzymes within the nonprolyl cis-peptide containing bacterial luciferase family," *Protein science*, vol. 14, no. 7, pp. 1840–1849, 2005.

[107] J. Chen and J. Xie, "Role and regulation of bacterial luxr-like regulators," *Journal of cellular biochemistry*, vol. 112, no. 10, pp. 2694–2702, 2011.

[108] M. B. Miller and B. L. Bassler, "Quorum sensing in bacteria," *Annual Reviews in Microbiology*, vol. 55, no. 1, pp. 165–199, 2001.

[109] A. V. Polkade, S. S. Mantri, U. J. Patwekar, and K. Jangid, "Quorum sensing: an under-explored phenomenon in the phylum actinobacteria," *Frontiers in microbiology*, vol. 7, p. 131, 2016.

[110] G. Walia and A. Surolia, "Insights into the regulatory characteristics of the mycobacterial dephosphocoenzyme a kinase: implications for the universal coa biosynthesis pathway," *PloS one*, vol. 6, no. 6, p. e21390, 2011.

[111] K. Li, T. Jiang, B. Yu, L. Wang, C. Gao, C. Ma, P. Xu, and Y. Ma, "Transcription elongation factor grea has functional chaperone activity," *PLoS One*, vol. 7, no. 12, p. e47521, 2012.

[112] G. M. Seibold and B. J. Eikmanns, "The glgx gene product of corynebacterium glutamicum is required for glycogen degradation and for fast adaptation to hyperosmotic stress," *Microbiology*, vol. 153, no. 7, pp. 2212–2220, 2007.

[113] W. Lin, V. Mathys, E. L. Y. Ang, V. H. Q. Koh, J. M. M. Gómez, M. L. T. Ang, S. Z. Z. Rahim, M. P. Tan, K. Pethe, and S. Alonso, "Urease activity represents an alternative pathway for mycobacterium tuberculosis nitrogen metabolism," *Infection and immunity*, pp. IAI–06 195, 2012.

[114] F. Zhang and J.-P. Xie, "Mammalian cell entry gene family of mycobacterium tuberculosis," *Molecular and cellular biochemistry*, vol. 352, no. 1-2, pp. 1–10, 2011.

[115] R. Plocinska, L. Martinez, G. Purushotham, E. Pandeeti, K. Sarva, E. Blaszczyk, J. Dziadek, M. Madiraju, and M. Rajagopalan, "Mycobacterium tuberculosis mtrb sensor kinase interactions with ftsi and wag31 proteins reveal a role for mtrb distinct from that regulating the mtra activities," *Journal of bacteriology*, pp. JB–01 795, 2014.

[116] G. Singh, G. Singh, D. Jadeja, and J. Kaur, "Lipid hydrolizing enzymes in virulence: Mycobacterium tuberculosis as a model system," *Critical reviews in microbiology*, vol. 36, no. 3, pp. 259–269, 2010.

[117] R. E. Haites, Y. S. Morita, M. J. McConville, and H. Billman-Jacobe, "Function of phosphatidylinositol in mycobacteria," *Journal of Biological Chemistry*, vol. 280, no. 12, pp. 10 981–10 987, 2005.

[118] G. Eulenburg, V. A. Higman, A. Diehl, M. Wilmanns, and S. J. Holton, "Structural and biochemical characterization of rv2140c, a phosphatidylethanolamine-binding protein from mycobacterium tuberculosis," *FEBS letters*, vol. 587, no. 18, pp. 2936–2942, 2013.

[119] P. K. Crellin, C.-Y. Luo, and Y. S. Morita, "Metabolism of plasma membrane lipids in mycobacteria and corynebacteria," in *Lipid Metabolism*. InTech, 2013.

[120] J. S. Blanchard, "Molecular mechanisms of drug resistance in mycobacterium tuberculosis," *Annual review of biochemistry*, vol. 65, no. 1, pp. 215–239, 1996.

[121] K. Charalambous, D. Miller, P. Curnow, and P. J. Booth, "Lipid bilayer composition influences small multidrug transporters," *BMC biochemistry*, vol. 9, no. 1, p. 31, 2008.

[122] D. Robins, "Phosphatidylethanolamine and lysophosphatidylethanolamine," *Journal of Pharmacy and Pharmacology*, vol. 15, no. 1, pp. 701–722, 1963.

[123] L. Blanc, M. Gilleron, J. Prandi, O.-r. Song, M.-S. Jang, B. Gicquel, D. Drocourt, O. Neyrolles, P. Brodin, G. Tiraby *et al.*, "Mycobacterium tuberculosis inhibits human innate immune responses via the production of tlr2 antagonist glycolipids," *Proceedings of the National Academy of Sciences*, vol. 114, no. 42, pp. 11 205–11 210, 2017.

[124] P. V. G. K. Sarma, L. Srikanth, K. Venkatesh, P. S. Murthy, and P. U. Sarma, "Isolation, purification and characterization of cardiolipin synthase from mycobacterium phlei {PRIVATE}," *Bioinformation*, vol. 9, no. 13, p. 690, 2013.

[125] Y. AKAMATSU and S. NOJIMA, "Separation and analyses of the individual phospholipids of mycobacteria," *The Journal of Biochemistry*, vol. 57, no. 3, pp. 430–439, 1965.

[126] Y. AKAMATSU, Y. ONO, and S. NOJIMA, "Phospholipid patterns in subcellular fractions of mycobacterium phlei," *The Journal of Biochemistry*, vol. 59, no. 2, pp. 176–182, 1966.

[127] B. E. Steinberg and S. Grinstein, "Pathogen destruction versus intracellular survival: the role of lipids as phagosomal fate determinants," *The Journal of clinical investigation*, vol. 118, no. 6, pp. 2002–2011, 2008.

[128] T. Yeung and S. Grinstein, "Lipid signaling and the modulation of surface charge during phagocytosis," *Immunological reviews*, vol. 219, no. 1, pp. 17–36, 2007.

[129] M. J. Sartain, D. L. Dick, C. D. Rithner, D. C. Crick, and J. T. Belisle, "Lipidomic analyses of mycobacterium tuberculosis based on accurate mass measurements and the novel mtb lipiddb," *Journal of lipid research*, pp. jlr–M010 363, 2011.

[130] J. Yao and C. O. Rock, "How bacterial pathogens eat host lipids: implications for the development of fatty acid synthesis therapeutics," *Journal of Biological Chemistry*, pp. jbc–R114, 2015.

[131] K. Takayama, C. Wang, and G. S. Besra, "Pathway to synthesis and processing of mycolic acids in mycobacterium tuberculosis," *Clinical microbiology reviews*, vol. 18, no. 1, pp. 81–101, 2005.

[132] M. Daffe, "Structure de l'enveloppe de mycobacterium tuberculosis," *Médecine et maladies infectieuses*, vol. 26, no. 11, pp. 891–897, 1996.

[133] K. Takayama, L. Wang, and H. L. David, "Effect of isoniazid on the in vivo mycolic acid synthesis, cell growth, and viability of mycobacterium tuberculosis," *Antimicrobial agents and chemotherapy*, vol. 2, no. 1, pp. 29–35, 1972.

[134] E. Tatar, S. ŞENKARDEŞ, H. E. Sellitepe, Ş. G. KÜÇÜKGÜZEL, Ş. A. KARAOĞLU, A. Bozdeveci, E. De Clercq, C. Pannecouque, T. B. HADDA, and İ. KÜÇÜKGÜZEL, "Synthesis, and prediction of molecular properties and antimicrobial activity of some acylhydrazones derived from *n*-(arylsulfonyl) methionine," *Turkish Journal of Chemistry*, vol. 40, no. 3, pp. 510–534, 2016.

[135] G. Sbardella, A. Mai, M. Artico, M. G. Setzu, G. Poni, and P. La Colla, "New 6-nitroquinolones: synthesis and antimicrobial activities," *Il Farmaco*, vol. 59, no. 6, pp. 463–471, 2004.

[136] M.-P. Collin, S. N. Hobbie, E. C. Böttger, and A. Vasella, "Synthesis of 1, 2, 3-triazole analogues of lincomycin," *Helvetica chimica acta*, vol. 91, no. 10, pp. 1838–1848, 2008.

[137] M. J. Smeulders, J. Keer, R. A. Speight, and H. D. Williams, "Adaptation of mycobacterium smegmatis to stationary phase," *Journal of bacteriology*, vol. 181, no. 1, pp. 270–283, 1999.

[138] J. Puffal, A. García-Heredia, K. C. Rahlwes, M. S. Siegrist, and Y. S. Morita, "Spatial control of cell envelope biosynthesis in mycobacteria," *Pathogens and disease*, vol. 76, no. 4, p. fty027, 2018.

[139] L. Chiaradia, C. Lefebvre, J. Parra, J. Marcoux, O. Burlet-Schiltz, G. Etienne, M. Tropis, and M. Daffé, "Dissecting the mycobacterial cell envelope and defining the composition of the native mycomembrane," *Scientific reports*, vol. 7, no. 1, p. 12807, 2017.

[140] A. Lemassu, A. Ortalo-Magne, F. Bardou, G. Silve, M.-A. Lanéelle, and M. Daffé, "Extracellular and surface-exposed polysaccharides of non-tuberculous mycobacteria," *Microbiology*, vol. 142, no. 6, pp. 1513–1520, 1996.

[141] A. F. Cunningham and C. L. Spreadbury, "Mycobacterial stationary phase induced by low oxygen tension: cell wall thickening and localization of the 16-kilodalton α-crystallin homolog," *Journal of bacteriology*, vol. 180, no. 4, pp. 801–808, 1998.

APPENDICES

A. TABLES

Table A.1.
Phage stocks

Number	Phage
1	LinStu
2	Crossroads
3	Pixie
4	Wee
5	Kugel & Avrafan
6	Chah
7	Babsiella
8	Kamiyu
9	L5
10	Patience
11	Giles
12	Henry
13	Omega
14	Papyrus
15	LHTSCC

Table A.2.
Babsiella annotated proteins identified by mass spectrometry

Protein	Function	Peptide Number	Spectra
gp4	portal protein	1	1
gp5		2	2
gp6	Protease	3	6
gp7	capsid protein	13	20
gp8		1	2
gp9		1	1
gp13		11	41
gp14	Tail assembly chaperone	3	3
gp16	Tape measure protein	5	9
gp17	minor tail protein	3	3
gp19	minor tail protein	8	10
gp21		3	4
gp26	Lysin A	11	20
gp27	Lysin B	4	4
gp50	FtsK domain protein	3	4
gp54	DNA methylase domain protein	1	1
gp73		2	2
gp75		3	4
gp76		9	16

Table A.3.: Chah annotated proteins identified by mass spectrometry

Protein	Function	Peptide Number	Spectra
gp1		1	1
gp7		2	11
gp9	Portal protein	2	2
gp10		1	1
gp12	Capsid protein	9	14
gp14		11	23
gp16		1	2
gp18	Major tail subunit	1	3
gp23		6	7
gp24		1	1
gp25		2	3
gp29	Tapemeasure protein	2	2
gp30		1	1
gp35		1	1
gp36		1	1
gp39		1	1
gp42		3	4
gp43		1	1
gp45		1	1
gp50	Lysin A	11	19
gp51	Lysin B	4	7
gp52		10	14
gp53		9	15
gp54	Helicase type III restriction	3	3
gp56		1	1

Table A.3 continued from previous page

Protein	Function	Peptide Number	Spectra
gp58		1	1
gp60	Helicase	12	20
gp61		2	2
gp63		4	4
gp68		4	6
gp69		1	1
gp73		6	10
gp74		3	4
gp93		3	3
gp94		4	5
gp99		2	3
gp102		2	2
gp103		1	1

Table A.4.

Giles annotated proteins identified by mass spectrometry

Protein	Function	Peptide Number	Spectra
gp3		2	2
gp7	Protease	4	8
gp8		2	3
gp9	Capsid subuint	6	7
gp10	Virion protein	8	15
gp15		1	1
gp16	Virion protein	7	20
gp18		1	1
gp20	Tapemeasure protein	1	1
gp24	Virion protein	1	1
gp31	Lysin A	1	2
gp32	Lysin B	3	5
gp36	Virion protein	1	1
gp37		2	4
gp53	RecT-like protein	2	2
gp58		2	2
gp59		1	1
gp60		1	1

Table A.5.: Henry annotated proteins identified by mass spectrometry

Protein	Function	Peptide Number	Spectra
gp13	Major capsid protein	14	29
gp15		1	2
gp19	Major tail subunit	6	13
gp21	Tail assembly chaperone	3	5
gp22	Tapemeasure protein	6	10
gp23		2	6
gp26	Minor tail subunit	3	5
gp27		6	9
gp30		2	3
gp33	Lysin A	8	14
gp34		4	11
gp35		2	3
gp36	Lysin B	2	2
gp37		1	1
gp49		1	2
gp57		2	3
gp64		2	3
gp67		1	1
gp89	RNA ligase	8	11
gp94		2	4
gp98	ClpP-like protease	9	19
gp109		1	2
gp111		3	4
gp112	DNA polymerase II	2	2
gp116		1	2

Table A.5 continued from previous page

Protein	Function	Peptide Number	Spectra
gp117	RecA	5	7
gp134		1	2
gp136		1	1

Table A.6.: LHTSCC annotated proteins identified by
mass spectrometry

Protein	Function	Peptide Number	Spectra
gp4	DNA polymerase III	4	4
gp7		3	6
gp8	Lysin A	11	18
gp9	Holin	3	5
gp10	Lysin B	4	7
gp11	Terminase large subunit	2	3
gp12	Portal protein	14	22
gp14	Scaffold protein	3	4
gp15	Capsid protein	18	74
gp17		3	6
gp18		1	1
gp22		1	1
gp23	Minor tail protein	8	13
gp24	Tail assembly chaperone	4	8
gp25	Tail assembly chaperone	5	6
gp26	Tapemeasure protein	9	11
gp27	Minor tail protein	2	2
gp28	Minor tail protein	1	1
gp32	Minor tail protein	4	5
gp46		1	3
gp50	Thymidylate synthase	5	8
gp51		4	9
gp52	Ribonucleotide reductase	11	15
gp54	RDF protein	4	4
gp57	DNA primase	1	1

Table A.6 continued from previous page

Protein	Function	Peptide Number	Spectra
gp74		1	1
gp82		1	1

Table A.7.: LinStu annotated proteins identified by mass
spectrometry

Protein	Function	Peptide Number	Spectra
gp29		3	4
gp62		2	4
gp70		2	2
gp77	L13E family domain protein	1	2
gp88		15	19
gp90		1	7
gp96	LysM domain	9	17
gp97		5	11
gp98		3	5
gp99		12	26
gp108		1	1
gp109		1	2
gp117		6	8
gp125		8	14
gp126		5	7
gp128	Tail assembly chaperone	1	2
gp130	Tapemeasure protein	1	1
gp138	Baseplate J	2	2
gp139		1	3
gp171		1	1
gp172		1	1
gp190		3	5
gp193		2	2
gp196		2	2
gp214	RusA	1	1

Protein	Function	Peptide Number	Spectra
gp216		9	20
gp220		5	6
gp221		1	1
gp225		2	2
gp234		6	8
gp243	Head decoration protein	6	7
gp247	Lysin A	3	3
gp248		3	5
gp249	Lysin B	2	2
gp263		3	3

Table A.7 continued from previous page

Table A.8.: Omega annotated proteins identified by mass spectrometry

Protein	Function	Peptide Number	Spectra
gp3	Terminase small unit	2	4
gp4	Enoyl-CoA-hydratase	1	1
gp15	Capsid protein	15	27
gp16	Glycosyltransferase	2	2
gp23		2	2
gp31	Major tail subunit	6	8
gp32	Tail assembly chaperones	3	5
gp35		4	4
gp36	Minor tail protein	2	2
gp37	Minor tail protein	1	1
gp38		2	3
gp39	D-ala-D-ala-carboxypeptidase	4	4
gp42		2	7
gp50	Lysin A	11	24
gp52		4	8
gp53	Lysin B	3	3
gp55		1	2
gp67		1	1
gp115		1	1
gp123	AddA-like protein	1	3
gp127	DNA methylase	2	3
gp144		5	9
gp149		1	1
gp160		1	1
gp162	RNA ligase	5	8

Protein	Function	Peptide Number	Spectra
gp163	Clp-like protease	2	2
gp164		2	3
gp173		5	8
gp174		3	6
gp198		1	1
gp211		2	2

Table A.9.
Papyrus annotated proteins identified by mass spectrometry

Protein	Function	Peptide Number	Spectra
gp2		2	4
gp7	Portal protein	3	4
gp14		3	4
gp15	Tail sheath	1	1
gp16		8	9
gp17	DNA binding domain protein	3	8
gp21		1	2
gp22		8	12
gp24	Fibronectin type III domain protein	2	4
gp25	Tail assembly chaperone	5	12
gp27	Tapemeasure protein	1	1
gp33		2	3
gp34		2	2
gp36		2	5
gp52		1	1
gp53		1	1
gp68		3	3
gp69		1	1
gp71		3	5
gp85		2	3
gp96		1	2

Table A.10.
Wee annotated proteins identified by mass spectrometry

Protein	Function	Peptide Number	Spectra
gp6	Major capsid protein	9	14
gp11	Major tail subunit	3	8
gp13	Tail assembly chaperone	2	2
gp31	Lysin A	2	3
gp32	Lysin B	2	2
gp71		1	4
gp102	Tail assembly chaperone	1	1

Table A.11.
Top ten proteins up-regulated by *M. smegmatis* exponential growing phase

Protein ID	Protein Names
I7FIV7	Multifunctional fusion protein [Includes: Sulfate adenylyltransferase subunit 1 (EC 2.7.7.4) (ATP-sulfurylase large subunit) (Sulfate adenylate transferase) (SAT); Adenylyl-sulfate kinase (EC 2.7.1.25) (APS kinase) (ATP adenosine-5'-phosphosulfate 3'-phosphotransferase) (Adenosine-5'-phosphosulfate kinase)]
A0QNJ0	ESX-1 secretion system ATPase EccB1
I7GBT0	Iron ABC transporter; periplasmic iron-binding protein
I7F6R1	Uncharacterized protein
A0R5I3	Transglycosylase
I7GS87	Endolytic murein transglycosylase (EC 4.2.2.-) (Peptidoglycan polymerization terminase)
A0QW23	Uroporphyrinogen decarboxylase (UPD) (URO-D) (EC 4.1.1.37)
I7G4H8	Phosphoglycerate mutase (EC 5.4.2.-)
I7GA30	Urease accessory protein UreG
A0QQB4	Isoniazid inductible protein IniA

Table A.12.
Top ten proteins up-regulated by *M. smegmatis* stationary growing phase

Protein ID	Protein Names
I7G7M8	Luciferase-like protein (EC 1.5.99.11)
I7FKV2	Uncharacterized protein
I7G914	tRNA pseudouridine synthase B (EC 5.4.99.25) (tRNA pseudouridine(55) synthase) (Psi55 synthase) (tRNA pseudouridylate synthase) (tRNA-uridine isomerase)
I7G5F5	Antibiotic biosynthesis monooxygenase
I7GAC1	PQQ-dependent dehydrogenase; methanol/ethanol family
A0QY55	Uncharacterized protein
I7G4N0	ABC transporter sugar-binding protein (EC 3.6.3.17)
I7G3H1	Uncharacterized protein
I7G1T7	Uncharacterized protein
I7FCD9	Conserved hypothetical alanine and proline rich protein

Table A.13.
Top ten proteins up-regulated by 4-hour incubation

Protein ID	Protein Names
I7FGY5	Phosphotyrosine protein phosphatase PtpA (EC 3.1.3.48)
I7G6N6	Diacylglycerol O-acyltransferase (EC 2.3.1.20)
I7FGM4	Uncharacterized protein
I7G7M8	Luciferase-like protein (EC 1.5.99.11)
I7G7E2	Uncharacterized protein
I7F6R1	Uncharacterized protein
I7GGE2	Secreted MPT51/MPB51 antigen protein fbpD
I7FCD9	Conserved hypothetical alanine and proline rich protein
I7GGN1	ABC transporter; permease protein
I7G165	Bifunctional protein PyrR [Includes: Pyrimidine operon regulatory protein; Uracil phosphoribosyltransferase (UPRTase) (EC 2.4.2.9)]

Table A.14.
Top ten proteins up-regulated by 10-hour incubation

Protein ID	Protein Names
I7FJ78	OsmC family protein
A0R1H2	Uncharacterized protein
A0R2F0	Tetratricopeptide repeat family protein
I7FC25	Short-chain dehydrogenase/reductase SDR (EC 1.1.1.275)
A0R217	Putative transcriptional regulator
A0QS18	Peptide chain release factor 3 (RF-3)
A0QR17	Glutamyl-tRNA reductase (GluTR) (EC 1.2.1.70)
I7FH77	Uncharacterized protein
I7F995	Ribulokinase (EC 2.7.1.16)
A0R0Y9	Elongation factor 4 (EF-4) (EC 3.6.5.n1) (Ribosomal back-translocase LepA)

Table A.15.
Top ten proteins up-regulated by FrenchFry infection

Protein ID	Protein Names
I7FH23	Transcriptional regulator; LuxR family
I7G1M3	Tryptophan synthase (EC 4.2.1.20)

Table A.16.

Top ten proteins down-regulated by FrenchFry infection

Protein ID	Protein Names
I7FH27	ABC sugar transporter; ATPase subunit (EC 3.6.3.-)
I7G535	Alcohol dehydrogenase; zinc-containing (EC 1.1.1.1)
I7GFI5	Divalent metal cation transporter MntH
I7GGN6	Uncharacterized protein
I7FJ78	OsmC family protein
I7FJC5	Uncharacterized protein
I7G7M8	Luciferase-like protein (EC 1.5.99.11)
I7GEP4	Putative transmembrane protein

Table A.17.

Top ten proteins up-regulated by MrGordo infection

Protein ID	Protein Names
I7FH47	Putative secreted protein
A0QUM5	Uncharacterized protein
I7G2J2	MCE-family protein MCE1c
I7FB52	4-coumarate CoA ligase (EC 6.2.1.12)
I7G174	Putative quinone oxidoreductase (NADPH:quinone oxidoreductase) (Zeta-crystallin) (EC 1.6.5.5)
A0QTK3	Sensor histidine kinase MtrB (EC 2.7.13.3)
I7G6W7	FO synthase
I7GFW3	ATP-dependent DNA helicase RecQ
I7G0N8	Phospho-2-dehydro-3-deoxyheptonate aldolase (EC 2.5.1.54) (3-deoxy-D-arabino-heptulosonate 7-phosphate synthase) (DAHP synthase) (Phospho-2-keto-3-deoxyheptonate aldolase)
A0QQT2	DNA or RNA helicase of superfamily protein II

Table A.18.

Top ten proteins down-regulated by MrGordo infection

Protein ID	Protein Names
I7F995	Ribulokinase (EC 2.7.1.16)
A0R2X1	Transcription elongation factor GreA (Transcript cleavage factor GreA)
A0QYE1	Urease subunit beta (EC 3.5.1.5) (Urea amidohydrolase subunit beta)
A0R597	Inorganic pyrophosphatase (EC 3.6.1.1) (Pyrophosphate phospho-hydrolase) (PPase)
A0R4K9	HIT family protein
I7GFV2	Glycogen debranching enzyme GlgX (EC 3.2.1.68)
A0QYE0	Urease subunit alpha (EC 3.5.1.5) (Urea amidohydrolase subunit alpha)
I7GFE7	Antibiotic biosynthesis monooxygenase
I7FJY5	Beta-lactamase (EC 3.5.2.6)
I7FFH5	Dephospho-CoA kinase (EC 2.7.1.24) (Dephosphocoenzyme A kinase)

Table A.19.

Biological processes that proteins up-regulated in exponential phase involved

Biological Processes
protein pupylation
cell division
transcription initiation from bacterial-type RNA polymerase promoter
metabolism
ribosome biogenesis
glycerol-3-phosphate metabolism
sulfate assimilation
biosynthesis
carbohydrate metabolism
protein targeting
regulation of sporulation
response to stress
nitrogen compound metabolism
nitrogen fixation
protein folding

Table A.20.

Cellular components that proteins up-regulated in exponential phase involved

Cellular Components
integral component of plasma membrane
fatty acid synthase complex
cell division site
extracellular space
periplasmic space

Table A.21.

Molecular functions that proteins up-regulated in exponential phase involved

Molecular Functions
nickel cation binding
2-hydroxy-3-oxoadipate synthase activity
heme binding
cyclohexanone monooxygenase activity
GTP cyclohydrolase II activity
biotin binding
structural constituent of ribosome
2-oxoglutarate decarboxylase activity
oxidoreductase activity
cysteine-glucosaminylinositol ligase activity
hydrolase activity
transferase activity
electron carrier activity
inositol-3-phosphate synthase activity
isomerase activity
ligase activity
catalytic activity
cofactor binding
iron-sulfur cluster binding
unfolded protein binding
lyase activity
sigma factor activity
transcription factor activity,sequence-specific DNA binding

Table A.22.

Biological processes that proteins up-regulated in stationary phase involved

Biological Processes
one-carbon metabolism
tRNA pseudouridine synthesis
polyamine transport
regulation of nitrogen utilization
response to stress
hydrogen peroxide catabolism
carbohydrate metabolism
metabolism
carbohydrate utilization
nitrogen fixation
protein folding

Table A.23.

Cellular components that proteins up-regulated in stationary phase involved

Cellular Components
periplasmic space
proteasome complex
integral component of membrane
extracellular region
cell
membrane

Table A.24.

Molecular functions that proteins up-regulated in stationary phase involved

Molecular Functions
coenzyme F420-dependent N5,N10-methenyltetrahydromethanopterin reductase activity
nickel cation binding
fatty acid O-methyltransferase activity
tRNA binding
hydrolase activity, acting on acid carbon-carbon bonds, in ketonic substances
ionotropic glutamate receptor activity
acetate-CoA ligase activity
maleimide hydrolase activity
proteasome binding
4-hydroxy-4-methyl-2-oxoglutarate aldolase activity
coenzyme binding
cofactor binding
oxidoreductase activity
structural constituent of ribosome
transcription factor activity, sequence-specific DNA binding
enzyme regulator activity
phosphoglucomutase activity
polyamine binding
transferase activity
2 iron, 2 sulfur cluster binding
carbohydrate binding
electron carrier activity
extracellular matrix binding
hydrolase activity
lyase activity

Table A.25.

Biological processes that proteins up-regulated in 4h incubation

Biological Processes
cell division
pseudouridine synthesis
metabolism
protein transport
hydrogen peroxide catabolism
response to oxidative stress
protein folding
nitrogen fixation
biosynthesis
protein polymerization

Table A.26.

Cellular components that proteins up-regulated in 4h incubation

Cellular Components
periplasmic space
phosphopyruvate hydratase complex
integral component of membrane
extracellular region
cell division site
cell surface

Table A.27.

Molecular functions that proteins up-regulated in 4h incubation

Molecular Functions
ferrous iron binding
tRNA binding
uracil phosphoribosyltransferase activity
biphenyl-2,3-diol
1,2-dioxygenase activity
cutinase activity
magnesium chelatase activity
biotin binding
cystathionine beta-synthase activity
L-ribulose-phosphate 4-epimerase activity
structural constituent of ribosome
oxidoreductase activity
4 iron, 4 sulfur cluster
binding
catalytic activity
cofactor binding
hydrolase activity
ligase activity
polyamine binding
transcription factor
activity, sequence-specific DNA binding
transferase activity

Table A.28.
Biological processes that proteins up-regulated in 10h incubation

Biological Processes
L-arabinose catabolism to xylulose 5-phosphate
cell wall organization
metabolism

Table A.29.
Cellular components that proteins up-regulated in 10h incubation

Cellular Components
DNA polymerase III complex
integral component of membrane

Table A.30.
Molecular functions that proteins up-regulated in 10h incubation

Molecular Functions
penicillin binding
translation release factor activity, codon specific
glutamyl-tRNA reductase activity
ribulokinase activity
GTPase activity
valine-tRNA ligase activity
enoyl-CoA hydratase activity
structural constituent of ribosome
ribosome binding
isomerase activity
oxidoreductase activity

Table A.31.

Cellular components that proteins down-regulated in FrenchFry infection

Cellular Components
integral component of membrane

Table A.32.

Molecular functions that proteins down-regulated in FrenchFry infection

Molecular Functions
coenzyme F420-dependent N5, N10-methenyltetrahydromethanopterin reductase activity
metal ion binding
metal ion transmembrane transporter activity
ATPase activity

Table A.33.

Biological processes that proteins up-regulated in FrenchFry infection

Biological Process
transcription, DNA-templated

Table A.34.

Molecular functions that proteins up-regulated in FrenchFry infection

Molecular Functions
pyridoxal phosphate binding
tryptophan synthase activity

Table A.35.
Biological processes that proteins down-regulated in MrGordo infection

Biological Processes
protein-pyridoxal-5-phosphate linkage via peptidyl-N6-pyridoxal phosphate-L-lysine
carbon fixation
metabolism
mycothiol-dependent detoxification
hydrogen peroxide catabolism
cell division
iron ion transport
ribosome biogenesis
S-adenosylmethionine biosynthesis
N-acetylglucosamine metabolism
carbohydrate metabolism
protein folding
biosynthesis
regulation of nitrogen utilization
cell adhesion
nitrogen fixation
pathogenesis
carbohydrate utilization
nitrogen compound metabolism
primary metabolism
pteridine-containing compound metabolism

Table A.36.

Cellular components that proteins down-regulated in MrGordo infection

Cellular Components
periplasmic space
bacterial nucleoid
glutamyl-tRNA(Gln) amidotransferase complex
cell
extracellular region
integral component of membrane
membrane
cell surface
outer membrane-bounded periplasmic space

Table A.37.
Molecular functions that proteins down-regulated in MrGordo infection

Molecular Functions
formyl-CoA transferase activity
3-ketosteroid 9-alpha-monooxygenase activity
isoamylase activity
phosphate ion binding
propionate-CoA ligase activity
L-cystine L-cysteine-lyase (deaminating)
steroid delta-isomerase activity
ionotropic glutamate receptor activity
antisigma factor binding
tRNA binding
potassium ion binding
galactose binding
polyamine binding
carbohydrate binding
2 iron, 2 sulfur cluster binding
sigma factor activity
enzyme regulator activity
protein tag
ribosome binding

Table A.38.

Biological processes that proteins up-regulated in MrGordo infection

Biological Processes
negative regulation of phosphate metabolism
dTDP-rhamnose biosynthesis
cell division
nitrogen compound transport
metabolism
ribosome biogenesis
response to antibiotic
protein pupylation
sulfate assimilation
biosynthesis
carbohydrate metabolism
protein folding
pathogenesis

Table A.39.

Cellular components that proteins up-regulated in MrGordo infection

Cellular Components
periplasmic space
integral component of membrane
cell wall
enterobactin synthetase complex
extracellular region
membrane
peroxisome

Table A.40.

Molecular functions that proteins up-regulated in MrGordo infection

Molecular Functions
manganese ion binding
cyclohexanone monooxygenase activity
fatty-acyl-CoA synthase activity
adenosylhomocysteinase activity
DNA replication origin binding
propionyl-CoA carboxylase activity
oxidoreductase activity
sirohydrochlorin ferrochelatase activity
branched-chain amino acid transmembrane transporter activity
phenylalanine racemase (ATP-hydrolyzing) activity
protein homodimerization activity
iron-sulfur cluster binding
cofactor binding
transcription factor
activity, sequence-specific DNA binding
electron carrier activity
isomerase activity
sigma factor activity
ribosome binding